Research on Physiological and Pathophysiological Functions of Chemokines for the Purpose of New Drug Development Targeting Chemokine Signaling in a Chronic Kidney Disease

May 2021

Naotoshi KANEMITSU

Research on Physiological and Pathophysiological Functions of Chemokines for the Purpose of New Drug Development Targeting Chemokine Signaling in a Chronic Kidney Disease

A Dissertation Submitted to
the School of the Integrative and Global Majors,
the University of Tsukuba
in Partial Fulfillment of the Requirements
for the Degree of Doctor of Philosophy in Medical Science
(Doctoral Program in Life Science Innovation)

Naotoshi KANEMITSU

Table of contents

Abstract

The immune system detects pathogens and irregular cells within the organism and protects it using innate and adaptive immune responses. Homeostasis of immune subsystems is maintained by a wide range of immune cells. Once the immune system detects pathogens, inflammatory cells and proteins are induced by the system, leading to inflammation. To produce these homeostatic and inflammatory status, various immune cells continuously migrate between lymphoid and non-lymphoid organs. This surveillance system of immune cells is coordinated by chemokines, proteins that induce immune cell migration and are responsible for homeostasis of immune systems and inflammatory reactions of the organism. Some chemokines are reportedly involved in immune dysfunctions in diseases such as autoimmune diseases and cancers. Therefore, modulating the pathophysiological functions of chemokines may be a new approach to drug development for certain diseases. To justify this approach, investigating physiological and pathophysiological functions of chemokines under several circumstances are considered crucial.

Chemokines induce biological functions by binding to cellular receptors.

Receptor-mediated signal transduction through chemokine receptors is important for lymphocyte trafficking across high endothelial venules (HEVs). However, the mode of action of individual chemokines expressed in the HEVs in lymphocyte trafficking remains unclear. In this study, CXCL13, a chemokine expressed in a substantial proportion of HEVs in both lymph nodes (LNs) and Peyer patches (PPs), was found to functions as an arrest chemokine for B cells. In a whole-mount analysis of mesenteric LNs (MLNs), B cells, unlike T cells, adhere poorly to HEVs of CXCL13-null mice. However, adhesion of B cells to the CXCL13-null HEVs is significantly restored when CXCL13 is added to the MLNs by superfusion. In *in vitro* studies, CXCL13 activated the small guanosine triphosphatase (GTPase) Rap1 in B cells, and a deficiency of RAPL, the Rap1 effector molecule, caused a substantial reduction in B-cell adhesion to intercellular adhesion molecule 1 (ICAM-1) under shear-resistant conditions. CXCL13 also activates α4 integrin in B cells and induces adhesion of B cells to mucosal addressin cell adhesion molecule 1 (MAdCAM-1). Accordingly, CXCL13 is identified as an arrest chemokine for B cells in HEVs and plays an important role in B-cell trafficking to PPs and MLNs.

As discussed above, some chemokines are agents of disease, which suggests that targeting chemokines may be an effective therapeutic approach. CXCL13

expression at tumor sites reportedly promotes migration of anti-tumor T cells expressing CXCR5. A combination treatment of CXCL13 and anti-PD-1-directed tumor therapy showed greater efficacy than their monotherapies in an animal study, suggesting that CXCL13 or a CXCR5 agonist could be a therapeutic option for tumor. However, it seemed difficult to pursue CXCL13/CXCR5-tageting drug development based on available in-house data and external reports after investigations of the chapter 1. On the other hand, other chemokines and their receptors are also known as a target of certain drugs. Several chemokines and their receptors-targeting drugs have been approved by the FDA: maraviroc (a CCR5 blocker for HIV-1 infection), plerixafor (a CXCR4 antagonist for non-Hodgkin's lymphoma and multiple myeloma), and mogamulizmab (an anti-CCR4 monoclonal antibody for mycosis fungoides or Sézary syndrome). In further investigations to seek chemokine-related targets, there are reports showing that CCL2 and its corresponding receptor, CCR2, are also involved in a wide variety of diseases, and a pathophysiological function of CCL2/CCR2 axis is considered one of the reasonable potential targets for drug development researches.

Glomeruli and renal tubule injury in chronic kidney disease (CKD) is reported to involve macrophage activation through interaction between CCL2 and

its receptor, CCR2. Studies of the effects of inhibiting CCL2/CCR2 signaling, using CCR2 inhibitors and anti-CCL2 antibodies, on kidney function in animals or humans with CKD have been reported. The activity of CCL2 is stabilized by replacement of its N-terminal glutamine with pyroglutamate (pE) by enzymes such as glutaminyl cyclase (QC) and isoQC. Through this process, pE-CCL2 becomes resistant to peptidases. I report here that inhibition of QC/isoQC using the QC/isoQC inhibitor PQ529 leads to the degradation of CCL2. This ameliorates CKD by reducing kidney inflammation in anti-glomerular basement membrane (GBM) antibody-induced glomerulonephritis in Wistar Kyoto (WKY) rats. Repeated oral administration of PQ529 (30 and 100 mg/kg, twice daily) for three weeks significantly reduced the CCL2 levels in serum and urine, and urinary protein excretion in a dose-dependent manner. The urinary protein and CCL2 levels in serum or urine were correlated. The expression of CD68, a macrophage marker, in the kidney cortex, and mononuclear infiltration into the tubulointerstitium, were reduced by the 3-week-treatment of PQ529. In addition, urinary KIM-1, β2 microglobulin, and clusterin levels decreased in PQ529-treated glomerulonephritis WKY rats, suggesting that inflammation in both the proximal and distal tubules was inhibited. It thus appears that PQ529 inhibits the progression of renal dysfunction by inhibiting the CCL2/CCR2 signaling. Inhibition of QC/isoQC may be a viable

alternative therapeutic approach for treating glomerulonephritis and CKD patients.

Abbreviations

CCL	C-C motif chemokine
CCR	C-C chemokine receptor
CXCL	C-X-C motif ligand
CXCR	C-X-C chemokine receptor
CKD	chronic kidney disease
GBM	glomerular basement membrane
GDS	guanosine diphosphate dissociation
GFP	green fluorescent protein
GST	glutathione S-transferase
HEVs	high endothelial venules
HGSC	high-grade serous ovarian cancer
H&E	hematoxylin and eosin
ICAM-1	inter cellular adhesion molecule 1
IgG	immunoglobulin G
isoQC	iso-glutaminyl cyclase
KIM-1	kidney injury molecule 1
LNs	lymph nodes

MAdCAM-1	mucosal addressin cell adhesion molecule-1
MLNs	mesenteric lymph nodes
PAS	periodic acid-Schiff
pE	pyroglutamate
PPs	Peyer patches
PTX	pertussis toxin
QC	glutaminyl cyclase
Rap1	Ras-associated protein 1
RAPL	regulator of adhesion and cell polarization enriched in lymphoid tissues
RBD	Ras-binding domain
WKY	Wistar Kyoto
WT	wild-type

General Introduction

The immune system protects an organism against disease. This system detects pathogens such as bacteria, viruses, or cancer cell, and then protects the organism using two major subsystems, innate and adaptive immunity, which exist in many species. However, dysfunctions of this immune system for some reasons result in disease conditions. Therefore, understanding both of physiological and pathophysiological conditions of this system, key mediators of these conditions, and mechanisms of the functions of the key mediator is considered crucial to find novel solutions of the treatment for certain diseases. Homeostasis of these immune subsystems are controlled by multiple immune cells and proteins. Once the innate immune system detects pathogens, inflammatory cells and proteins are induced by the system. For both homeostatic and inflammatory states, the continuous migration of immune cells from lymphoid organs to sites of infection is key. Chemokines are a well-known protein family that induces multiple immune cell migrations. Given chemokines' essential physiological and pathophysiological roles in the immune system, in general, development of novel drugs targeting certain chemokine and chemokine signaling has been expected to lead to new treatments for certain diseases.

Chemokines generally consist of 70-125 amino acids with a molecular weight of 6-14 kDa (Le et al. 2004). They have different subfamilies, CCL, CXCL, XCL, and CX3CL, which are determined by the positioning of the first two of four conserved cysteine residues (Schulz et al. 2016). Functions, and the genomic and chromosomal organizations of chemokines, is moderately conserved between species. In humans, 27 CCL, 17 CXCL, 2 XCL, and 1 CX3CL chemokines have been identified, while in mice, 22, 15, 1, and 1, respectively, have been identified (Schulz et al. 2016). Chemokines bind to chemokine receptors expressed on all immune cells and a wide variety of non-immune cells, leading to biological functions in these cells. These receptors are a receptor superfamily of seven transmembrane-spanning heterotrimeric G protein-coupled receptor. Twenty signaling and 5 of non-signaling chemokine receptors have been identified (Schulz et al. 2016).

CXCL13, also known as BLC (B-lymphocyte chemoattractant) or BCA-1 (B cell-attracting chemokine 1), is classified as one of the CXCL chemokines. This chemokine is broadly expressed by stromal cells in B-cell areas of secondary lymphoid tissues, such as lymph nodes, Peyer's patches, spleen, and tonsils. CXCL13 functions as a homeostatic chemokine through its corresponding receptor,

CXCR5, originally known as Burkitt's lymphoma receptor 1 (BLR1) (Hussain et al. 2019). CXCR5 is also broadly expressed on mature B cells, a part of follicular helper T cells, and skin-derived migratory dendritic cells. CXCL13/CXCR5 axis reportedly control CXCR5-expressing cells' migration into secondary lymphoid organs. However, detailed mechanisms of physiological functions of CXCL13/CXCR5 axis in B cell migration to secondary lymphoid organs remained unknown. Therefore, in the chapter 1, investigations on a physiological function of CXCL13 as an arrest chemokine in B lymphocyte homing were firstly conducted and described.

Although chemokines and chemokine receptors reportedly play major functions in homeostasis of the immune system, including leukocyte trafficking/homing and inflammation (Rot et al. 2004, Miyasaka et al. 2004), it has recently been reported that their aberrant functions are implicated in immune diseases, kidney dysfunctions, angiogenesis, and cancer progressions (Cheng et al. 2014, Griffith et al. 2014, Schulz et al. 2016, Cecchinato et al. 2016, Castan et al. 2017, Nagarsheth et al. 2017, Chen et al. 2018). Accordingly, modulating chemokine and chemokine receptor signaling may be one strategy for treating certain diseases (Solari et al. 2014). In fact, there have been several approved anti-

chemokine receptor treatments, including maraviroc, an antagonist for CCR5 for treatment of HIV infection (Moore et al. 2009, Stellbrink et al. 2016); plerixafor, a small-molecule CXCR4 antagonist used in combination with granulocyte colony-stimulating factor (GCSF) to mobilize haematopoietic stem cells to the peripheral blood for collection and subsequent autologous transplantation in patients with non-Hodgkin's lymphoma and multiple myeloma (DiPersio et al. 2009, Steinberg et al. 2010); and mogamulizmab, a monoclonal-antibody CCR4 antagonist for the treatment of mycosis fungoides or Sézary syndrome (Kim et al. 2018, Kasamon et al. 2019). Further study of anti-chemokine therapy is warranted (Miao et al. 2020) as there remain many other diseases associated with dyshomeostasis of the immune system. To develop safe, efficacious drugs to manipulate chemokine signaling, a greater understanding of the physiological and pathophysiological functions of these proteins is essential.

While aberrant CXCL13/CXCR5 function is reportedly involved in several diseases such as advanced cancers, rheumatoid arthritis, Sjögren's disease, and multiple sclerosis (Yang et al. 2021, Hussain et al. 2019), CXCL13 has been demonstrated basically as a homeostatic chemokine. As far as literature surveys and in-house experimental researches, there were also insufficient strong rationales to

support further studies on drug development modulating CXCL13/CXCR5 axis. On the other hand, chemokine-based drug development remained warranted, given other successful examples of other FDA-approved chemokine-related drugs as described above, further researched on another arrest chemokine, CCL2, and its pathophysiological functions for the purpose of drug development was continued in the chapter 2.

CCL2, originally known as monocyte chemoattractant protein-1 (MCP-1), is one of the CC chemokine subfamily. CCL2 is expressed in a wide variety of cells such as macrophages, monocytes, microglial cells, astrocytes, mesangial cells, fibroblasts, endothelial cells, epithelial cells, and smooth muscle cells. This chemokine functions by its ligation to a corresponding receptor, CCR2 (Moadab et al. 2021). As well as a function of arrest chemokine of CXCL13 to B cells as investigated in the chapter 1, CCL2 is also reportedly one of arrest chemokines expressing on HEVs and inflammatory sites to monocytes (Ley. 2003). In addition to the role of an arrest chemokine in monocyte trafficking and migration, CCL2 shows multiple roles in immune system through its chemoattractive function to CCR2-expressing immune and non-immune cells in immune homeostasis. On the other hand, this chemokine also participates in inflammatory responses and other

diseases such as cancer and chronic kidney diseases (CKD). Pathophysiological functions of CCL2/CCR2 axis reportedly plays a crucial role in these diseases. Several investigations showed that CCL2/CCR2 axis could be one of the reasonable targets for novel drug development. In human CKD, involvement of elevated CCL2 has already been known (Wada et al. 2000, Tesch et al 1999, Giunti et al. 2010, Tampe et al. 2014, Haller et al. 2016, Moreno et al. 2018). Modulating the function of CCL2/CCR2 has been considered promising approaches to treat CKD (DeZeeuw et al. 2015, Menne et al. 2017). In the chapter 2, a novel approach to decrease CCL2 levels in CKD by inhibiting QC/isoQC, was investigated to evaluate an approach of modulating pathophysiological function of CCL2 as a novel treatment for CKD.

Chapter 1: CXCL13 is an arrest chemokine for B cells in high endothelial venules

Introduction

A wide range of experiments has revealed that a variety of chemokines are produced at the target sites of leukocyte trafficking and homing (Rot et al. 2004, Miyasaka et al. 2004). These chemokines are chemoattractants for leukocytes expressing the corresponding chemokine receptors. In addition to this activity, certain chemokines localized to the venular wall induce the integrin-mediated arrest of leukocytes rolling on the venular wall ("arrest"), thereby facilitating firm leukocyte adherence to the venular endothelium. This is essential for the recruitment of leukocytes to secondary lymphoid tissues or inflammation sites (Rot et al. 2004, Miyasaka et al. 2004). It has been reported that CCL21 plays a crucial role in the migration of naïve T cells to LNs and PPs (Stein et al. 2000, Warnock et al. 2000). CCL21 is expressed on the luminal surface of HEVs (Stein et al. 2000). Desensitization of CCR7, a corresponding receptor for CCL21, leads to severe impairment of integrin (leukocyte function–associated antigen 1 [LFA-1])-mediated T-cell arrest at HEVs (Stein et al. 2000, Warnock et al. 2000). Mice

congenitally lacking CCL21 and CCL19 (*plt/plt* mice), show severely impaired T-cell arrest at HEVs (Nakano et al. 2001). Additionally, T-cell arrest is restored by the reconstitution of expression of CCL21 (Stein et al. 2000). Ley has proposed a definition of an arrest chemokine as one that: (1) is luminally expressed; (2) has arrest activity that is eliminated by blocking the function of the chemokine or its receptor; and (3) has its arrest function restored by reconstitution of the expression of chemokines on endothelial cells (Ley. 2003). On this basis, CCL21 is considered an arrest chemokine for naïve T cells. The biological mechanism of CCL21-induced arrest is the triggering of signal transduction pathways involving Rap1 and RAPL (Shimonaka et al. 2003, Katagiri et al. 2003). RAPL-deficient mice do indeed show impaired trafficking of T cells, B cells, and dendritic cells (Katagiri et al. 2004). CCL7 has been identified as a T cell-arrest chemokine, but an arrest chemokine for B cells at HEVs has not been reported. Chemokine signals through CXCR4 and CCR7 are important for B-cell entry into LNs, and CXCR4, CCR7, and CXCR5 are important for entry into PPs (Okada et al. 2002). However, detailed mechanisms of these chemokine signals have remained unclear. The ligand for CXCR5 is CXCL13, which shows a selective chemoattractant function to mature B cells (Gunn et al. 1998) and a subset of T cells (Schaerli et al. 2000). CXCL13-deficient mice show defects in development of peripheral LNs and PPs, but not MLNs

(Ebisuno et al. 2003, Ansel et al. 2000). B-cell trafficking in MLNs was impaired as well (Ebisuno et al. 2003). It also has been reported that: (1) CXCL13 is luminally expressed in approximately 50% of the HEVs in LNs and PPs; (2) CXCL13-deficient PP HEVs show much reduction in B-cell adhesion compared with T-cell adhesion; and (3) reconstitution of CXCL13 expression by superfusion of CXCL13 in CXCL13-deficient PPs significantly restores B-cell arrest in PP HEVs (Ebisuno et al. 2003). This indicates that CXCL13 plays an essential role in B-cell arrest at the HEVs of PPs. What remains unclear is the mode of action of the CXCL13 for B cells and the roles of CXCL13 expressed in LN HEVs in B-cell arrest. In this study, the mode of action of CXCL13 on B cells in MLN HEVs was investigated using CXCL13-deficient mice and found that CXCL13 is an arrest chemokine for B cells at HEVs. Additionally, it was found that CXCL13 activates signal transduction pathways through Rap1 and RAPL, resulting in integrin activation in B cells.

Materials and Methods

Animals

Animals used in this study are described in Kanemitsu et al. 2005. C57BL/6 mice (Japan SLC, Hamamatsu, Japan) and green fluorescent protein (GFP)–transgenic mice (Okabe et al. 1997) were kindly provided by Dr. M. Okabe of Osaka University. The mice were housed under specific pathogen-free conditions. CXCL13-KO mice and RAPL-KO mice were established and used as described previously (Katagiri et al. 2004, Ebisuno et al. 2003). Our experimental protocol was approved by the Ethics Review Committee for Animal Experimentation of Osaka University Medical School.

Lymphocyte Isolation and antibodies

Lymphocyte isolation was conducted as described in Kanemitsu et al. 2005. Used antibodies were also described in Kanemitsu et al. 2005. B cells and T cells were isolated by incubating spleen cells with a mixture of anti-CD3 and anti-CD11b monoclonal antibodies (mAbs) or anti-B220 and anti-CD11b mAbs, respectively, followed by AutoMACS separation (Milte-nyi Biotec, Bergisch Gladbach, Germany), as described previously (Ebisuno et al. 2003). The purity of the B and T

cells was more than 90%, on average, as determined by flow cytometry. The MECA-89 mAb17 was purified from ascites and labeled with Alexa Fluor 594 or Alexa Fluor 647 (Molecular Probes, Eugene, OR). Unless otherwise noted, the origins of the antibodies used in this study were the same as reported previously (Ebisuno et al. 2003).

Whole-mount microscopy

Whole-mount microscopy assay was conducted as described in Kanemitsu et al. 2005. Purified B cells and T cells from GFP-transgenic mice were resuspended in warm saline and injected intravenously into wild-type (WT) and CXCL13-KO mice (n = 3; 1 x 10^7 cells/mouse). Ten minutes after the lymphocyte injection, Alexa Fluor 594- or Alexa Fluor 647-labeled MECA-89 mAb was injected intravenously to label the mucosal addressin cell adhesion molecule 1-positive (MAdCAM-1^+) HEVs in situ. Mice were humanely killed 15 minutes after the lymphocyte injection and perfused with saline and 4% paraformaldehyde in phosphate-buffered saline (PBS). The MLNs were collected, fixed with 4% paraformaldehyde, and treated with increasing concentrations of saccharose (10%, 20%, and 30%). Cell adhesion to MAdCAM-1^+ MLN HEVs was analyzed by confocal microscopy (LSM510META; Carl Zeiss, Jena, Germany, or Randiance 2100; Bio-Rad,

Hercules, CA). Digital images were processed using Photoshop 6.0 software (Adobe Systems, San Jose, CA). For quantification of the lymphocyte adhesion to HEVs, the number of lymphocytes that adhered to each HEV segment and the length of the HEV segments were evaluated for 80 HEV segments/mouse. Superfusion with mouse CXCL13 (Dako, Glostrup, Denmark; 25 μg/mL in PBS for 90 minutes) and immunohistochemical analyses were performed as described previously (Ebisuno et al. 2003). In some experiments, purified B cells were preincubated with pertussis toxin (PTX; 100 ng/mL; Calbiochem, San Diego, CA) at 37°C for 2 hours, washed, and injected intravenously into mice.

Static adhesion assay

Static adhesion assay was conducted as described in Kanemitsu et al. 2005. Multiwell (4-mm diameter) glass slides were coated with rat intercellular adhesion molecule 1 (ICAM-1)/IgG (Mukasa et al. 1999) (a gift from Dr. Y. Iigo, Daiichi Pharmaceutical, Tokyo, Japan), rat MAdCAM-1/IgG (Iizuka et al. 2000), or human IgG (50 ng/well) overnight at 4°C and then blocked with fetal calf serum. B cells (1×10^5) were then added and allowed to settle for 15 minutes at 37°C. Subsequently, mouse CXCL13 (Dako) was added to the wells and incubated for 5 minutes at 37°C to induce cell adhesion. Phorbol myristate acetate (PMA; final concentration of 25

ng/mL; Sigma-Aldrich, St Louis, MO) was used as a positive control of adhesion. After unbound cells were washed off, the bound cells were counted. For antibody blocking, the cells or immobilized ligands were preincubated with a mAb or a control antibody for 30 minutes at 37°C. Anti–mouse CD11a (KBA) (Nishimura et al. 1988), anti–rat CD54 (1A29) (Tamatani et al. 1990), and anti–rat MAdCAM-1 (OST2) (Iizuka et al. 2000) were used at 20 μg/mL, whereas anti-CD49d (PS/2) (Miyake et al. 1991) was used as a hybridoma culture supernatant. In some experiments, cells were preincubated with PTX (100 ng/mL) at 37°C for 15 minutes, washed, and used in binding studies.

Detachment assay

Detachment assay was conducted as described in Kanemitsu et al. 2005. ICAM-1/IgG (10 μg/mL) and CXCL13 (2 μM) were immobilized on the inside walls of a glass capillary tube (ϕ: 0.69 mm; Drummond, Broomal, PA), as previously described (Campbell et al. 1998), so that the upstream half of each tube was coated with ICAM-1/IgG alone and the downstream half was coated with ICAM-1/IgG plus CXCL13. B cells (1 x 10^6 cells/mL) were injected into the capillary tubes at 0.25 dynes/cm^2 for 5 minutes at 37°C. Shear stress was generated with an automated Harvard syringe pump (PHD2000; Instech Laboratories,

Plymouth Meeting, PA). The flow was then increased in 2-fold increments every 20 seconds. The experiments were videotaped for analysis and the number of B cells that remained bound at each interval was counted. In some experiments, cells were treated with PTX or KBA (see "Static adhesion assay"). For the functional comparison of wild-type and RAPL-deficient B cells, shear-resistant B-cell adhesion to immobilized ICAM-1/IgG (0.5 μg/mL) was assessed in a parallel flow chamber, as described (Shimonaka et al. 2003).

Flow adhesion assay

Flow adhesion assay was conducted as described in Kanemitsu et al. 2005. MAdCAM-1/IgG or CXCL13 was immobilized on glass capillary tubes as described for the static adhesion assay. B cells (1 x 10^6 cells/mL) were then injected into the capillary tubes at 1.0 dyne/cm^2 at 37°C and images were recorded with a cell-viewing system (SRM-100; Nikon, Tokyo, Japan) and video recorder (BR-S600; Victor, Yokohama, Japan) using a Nikon Plan Fluor DL 10 x/0.3 numeric aperture objective. Digital images were prepared using Quick Time 6.5.2 (Apple, Cupertino, CA) and Adobe Photoshop 6.0. Three categories of B-cell tethers under continuous flow were determined, as described previously (Shamri et al. 2002): "transient" if the cells attached briefly (<3 seconds) to the substrate; "rolling" if

cells rolled on the substrate at least 3 seconds; and "arrested" if cells were arrested on the substrate and remained adherent and stationary for at least 20 seconds. All cellular interactions were determined by manually tracking individual cells in a 0.39-mm^2 area for 1 minute. For the blocking of MAdCAM-1, the tubes were pretreated with OST2 (20 μg/mL) for 30 minutes at room temperature. In some experiments, B cells were preincubated with PS/2 or PTX (see "static adhesion assay").

Detachment assay with cultured endothelial cells

Detachment assay with cultured endothelial cells was conducted as described in Kanemitsu et al. 2005. BC1 mouse endothelial cells were derived from the cortical bone of BALB/c mice (Zhang et al. 1998) and used in detachment assays under flow, as previously described (Shimonaka et al. 2003). A monolayer of BC1 cells was grown on a gelatin-coated plastic dish and placed in a flow chamber (Glycotech, Gaithersburg, MD). The endothelial cell monolayer was preincubated with 1μM CXCL13 for 5 minutes and then unbound CXCL13 was removed by gentle washing. B cells (5 x 10^6/mL) were injected into the chamber at 0.1 dyne/cm^2 for 8 minutes. Next, a higher shear stress (2 dynes/cm^2) was applied for 10 minutes (Shimonaka et al. 2003). Experiments were videotaped for analysis,

and the number of adherent B cells was counted. In blocking experiments, B cells were pretreated with PTX, KBA, or PS/2, as described for whole mount microscopy.

Rap1 activation

Rap1 activation was evaluated as described in Kanemitsu et al. 2005. Purified B cells were stimulated with 30 nM mouse CXCL13 at 37°C for the indicated time periods. The cells (1 x 10^7) were lysed in ice-cold lysis buffer (50 mM Tris [tris(hydroxymethyl)aminomethane]–HCl, pH 7.4, containing 500 mM NaCl, 1% NP-40, 2.5 mM $MgCl_2$, 10% glycerol, 10 μg/mL aprotinin, and 10 μg/mL leupeptin) and subjected to a pull-down assay using a glutathione S-transferase (GST)-tagged Ral guanosine diphosphate dissociation stimulator (GDS)-Ras-binding domain (RBD) fusion protein coupled to glutathione-agarose beads, as previously described (Reedquist et al. 1998). Rap1 protein was detected by Western blotting using an anti-Rap1 antibody (BD PharMingen, San Diego, CA).

Results

Adhesion of B cells to MLN HEVs is significantly reduced in CXCL13-KO mice and is restored by the reconstitution of expression of CXCL13

First, B-cell adhesion was quantified in the MLN HEVs of CXCL13-KO and WT mice. For this purpose, GFP-transgenic B and T cells were injected into CXCL13-KO and WT mice, and their behavior in HEVs, assessed using whole-mount microscopy of the MLNs, was observed 15 minutes after the injection. As shown in Figure 1-1A, some B cells were detected on the walls of MLN HEVs in WT mice, but this number was reduced 60% in CXCL13-KO mice (Figure 1-1B). The frequency distribution of binding B cells per HEV segment was shifted to the left in the CXCL13-KO mice relative to the WT mice (Figure 1-1C), showing that the adhesion of B cells to the MLN HEVs was significantly reduced in the absence of expression of CXCL13. In contrast, the number of T cells binding to the MLN HEVs was similar for both the CXCL13-KO and WT mice (Figure 1-1A-B). These findings indicated that the reduction in adhesion of B cells was not caused by secondary effects such as a difference in the blood flow rate in the HEVs of these mice. However, it should also be noted that there was a small, but significant, level of B-cell adhesion in the CXCL13-KO HEVs (Figure 1-1A-B) and this B-cell

adhesion was almost completely inhibited by the treatment of B cells with PTX, a Gαi-specific inhibitor (data not shown). This result indicated that CXCL13 is not the only chemokine regulating B-cell adhesion in LN HEVs.

Then, CXCL13 was topically applied to the MLNs of CXCL13-KO mice. This reconstituted expression of CXCL13 and significantly restored B-cell adhesion in CXCL13-KO MLN HEVs (Figure 1-1D). These observations indicate that CXCL13 plays an essential role in B-cell arrest to MLN HEVs.

CXCL13 promotes binding of B cells to immobilized ICAM-1 and MAdCAM-1 under both static and flow conditions

To understand the mode of action of CXCL13 on B cells, it was investigated whether CXCL13 could induce integrin-mediated binding of B cells to ICAM-1 and MAdCAM-1, the HEV-associated endothelial ligands. CXCL13 significantly induced B-cell adhesion to ICAM-1 (Figure 1-2A) and MAdCAM-1 (Figure 1-2B) under static conditions, showing bell-shaped dose-response curves that are typical for chemotactic responses to chemokines. The CXCL13-induced binding of B cells to ICAM-1 was specifically blocked by an anti-CD11a or anti-ICAM-1 mAb (Figure 1-2C). The B-cell adhesion to MAdCAM-1 induced by treatment of

CXCL13 was also specifically blocked by an anti-CD49d or anti-MAdCAM-1 mAb (Figure 1-2D). A PTX almost completely inhibited the CXCL13-induced B-cell binding to ICAM-1 (Figure 1-2E) and MAdCAM-1 (Figure 1-2F). These results indicate that CXCL13 induces adhesion of B cells mainly via Gαi-dependent, integrin-dependent signal transduction pathways.

Next, it was tested if CXCL13 induces B-cell adhesion to ICAM-1 under shear stress conditions. B cells were first allowed to interact with immobilized ICAM-1 at low shear stress and then subjected to continuously increasing stress. While most of the B cells that initially adhered to the immobilized ICAM-1 detached with increments of shear stress, the majority of B cells remained binding to ICAM-1 co-immobilized with CXCL13, even at the highest shear stress examined (16 dyne/cm^2) (Figure 1-3A). The increased B-cell adhesion was inhibited by PTX to the basal level (Figure 1-3B), and also by anti-CD11a mAb (data not shown), demonstrating that CXCL13 activated LFA-1 on B cells via PTX-dependent signal transduction, and induced shear-resistant B-cell adhesion to ICAM-1. CXCL13 promoted arrest of B cells on MAdCAM-1 in a dose-dependent manner under physiologic flow conditions (1 dyne/cm^2), although it did not significantly alter the total number of B cells interacting with the immobilized

MAdCAM-1 (Figure 1-4A). In the absence of CXCL13, almost no B-cell arrest on MAdCAM-1 was observed, whereas it was observed in the presence of CXCL13 (Figure 1-4B). The B-cell adhesion induced by CXCL13 was almost completely inhibited by an anti-MAdCAM-1 mAb applied to the capillary tube (Figure 1-4C), by an anti-CD49 mAb, and by PTX to the B cells (Figure 1-4D). Similar inhibition was not observed in treatment with the control IgG, indicating that CXCL13 activates the α4 integrin on B cells to bind to MAdCAM-1 to induce B-cell arrest under physiologic flow conditions.

CXCL13 promotes shear-resistant B-cell adhesion to an endothelial cell monolayer

Then, the effects of CXCL13 on shear-resistant adhesion of B cells to a BC1 endothelial cell monolayer was investigated. When CXCL13 was pretreated to the BC1 monolayer, more than 60% of the input B cells remained binding to the BC1 monolayer under high-shear stress flow conditions, whereas when culture medium alone was pretreated to the monolayer, only approximately 30% of the input B cells were attached under the same flow conditions (Figure 1-5). PTX, anti-CD11a mAb, and anti-CD49d mAb inhibited the B-cell adhesion to basal levels under shear stress conditions, and the combination of anti-CD11a and anti-CD49d almost completely inhibited the CXCL13-induced adhesion. These results indicated that CXCL13

promoted LFA-1- and α4 integrin-dependent B-cell binding to the BC1 monolayer. Supporting this finding, the BC1 cells expressed both ICAM-1 and vascular cell adhesion molecule 1 (VCAM-1) and showed a detectable level of CXCL13 binding in a flowcytometry (data not shown). Therefore, these results demonstrate that CXCL13 activates both LFA-1 and α4 integrins on B cells, inducing B-cell adhesion to endothelial cells under shear stress conditions.

CXCL13 rapidly activates Rap1 and requires RAPL for its integrin activation in B cells

Finally, CXCL13 signal-transduction pathways leading to integrin activation in B cells was studied. Because it has been reported that Rap1 is implicated in the chemokine-induced integrin activation in lymphocytes (Shimonaka et al. 2003), Involvement of Rap1 in CXCL13-induced integrin activation in B cells was examined by a pull-down assay using a GST-Ral GDS fusion protein. CXCL13 activated Rap1 in B cells at 30 seconds (Figure 1-6A), and then it was downregulated to basal levels within 5 minutes. To further understand the mode of action of Rap1 activation in B-cell adhesion to integrin ligands, the contribution of RAPL (Katagiri et al. 2003, Katagiri et al. 2004), an effector molecule of Rap1, was evaluated in CXCL13-induced B-cell adhesion. B cells

lacking RAPL showed significantly decreased levels of shear-resistant adhesion to ICAM-1 compared to WT B cells (Figure 1-6B). However, RAPL deficiency did not completely inhibit adhesion, indicating that RAPL-independent mechanisms also function in B-cell adhesion. The expression level of LFA-1 on the B cell surface in RAPL-KO B cells was similar to that of WT B cells (data not shown). These observations show that CXCL13 activates Rap1 and RAPL-dependent signal-transduction pathways in integrin activation in B cells.

Discussion

CXCL13, which is broadly expressed by HEVs in LNs and PPs (Ebisuno et al. 2003), plays the role of an arrest chemokine for B cells in MLNs. It was found that adhesion of B cells in MLN HEVs was selectively impaired in CXCL13-deficient mice and was significantly restored by the reconstitution of the expression of CXCL13. Additionally, CXCL13 induced integrin-dependent shear-resistant B-cell adhesion *in vitro*. CXCL13-induced activation of integrin in B cells depended on Gαi and involved activation of Rap1/RAPL-mediated signal pathway. These results show that CXCL13 plays an essential role in the arrest of B cells in both MLN HEVs and PP HEVs.

It has been reported that B-cell adhesion was significantly reduced in CXCL13-KO MLN HEVs compared with that in WT mice. Although a deficiency of CXCL13 significantly influences the development of secondary lymphoid tissues (Ansel et al. 2000), it has relatively little influence on the MLNs. In CXCL13-KO mice, the HEVs are normally found there and the CXCL13-KO HEVs express CCL21, CXCL12, and MAdCAM-1 at levels comparable to those in WT mice (Y. E. and T. Tanaka, unpublished observation, June 2003). When interactions between

B cells and HEVs of comparable sizes and lengths in CXCL13-KO and WT mice were quantified, the adhesion of B cells to HEVs in the CXCL13-KO mice was found to be significantly lower than that in the WT mice, suggesting that this reduction was likely due to the deficiency of CXCL13 in HEVs but not to secondary effects induced by lack of the expression of CXCL13, such as changes in HEV structure and/or blood flow. The deficiency of B-cell adhesion in CXCL13-KO MLN HEVs is consistent with previous reports that the number of B-cells migrating into the MLNs was significantly reduced in CXCL13-KO mice in a short-term *in vivo* lymphocyte migration assay (Ebisuno et al. 2003). There also is a report that CXCL13 is required for B-cell trafficking into PPs, but not LNs (Okada et al. 2002). It should be noted that the trafficking of WT B cells in CXCL13-KO mice was examined in this study, whereas Okada et al. (Okada et al. 2002) studied B-cell trafficking in cells lacking CXCR5 in WT mice. One explanation for the difference between these two reports is that a CXCR5 deficiency results in compensatory changes in B-cell responses to chemokines other than CXCL13, and these changes may have masked the functional significance of CXCL13 in LN HEVs. This possibility should be verified in future studies. It should also be noted that CXCL13 is not the sole chemokine triggering B-cell adhesion to HEVs because there is a low, but readily detectable, level of B-cell adhesion in the MLN HEVs in CXCL13-KO

mice. Another study demonstrated that multiple chemokines are involved in B-cell entry into LNs and PPs via HEVs (Okada et al. 2002). It was shown that CCL21, CCL19, and CXCL12, in addition to CXCL13, are expressed in substantial portions of the HEVs in LNs and PPs (Ebisuno et al; Y.E., unpublished observation, June 2003). Therefore, it will also be important to determine how these chemokine signals influence each other and regulate B-cell adhesion to, and transmigration across, HEVs. With regard to the CXCL13-CXCR5 signal pathways, activation of Rap1 was rapidly induced in B cells by stimulation with CXCL13. Together with a report that activation of Rap1 was also observed in CXCL12-stimulated B cells (McLeod et al. 2002), these results indicate, as in T cells (Shimonaka et al. 2003), an essential role of Rap1-dependent signal transductions in the chemokine-induced integrin activation of B cells. Additionally, B cells lacking RAPL, an effector molecule of Rap1, showed severely reduced levels of shear-resistant adhesion to ICAM-1 and significantly impaired trafficking to LNs (Katagiri et al. 2004). Deficiency of RAPL, however, did not completely abrogate CXCL13-induced shear-resistant B-cell binding, suggesting the existence of an alternative mechanism in CXCL13-induced integrin activation in B cells. To elucidate mechanisms of CXCL13-triggered integrin activation more fully in B cells, additional studies will be required.

This study showed that CXCL13 rapidly activates multiple integrins in B cells, including LFA-1 and α4 integrin, and that this activation is Gαi-dependent. Shamri et al. also have reported activation of multiple integrins in lymphocytes by signaling through chemokine receptors (Shamri et al. 2002). Signaling through CXCR4 or CCR7 activates both LFA-1 and α4 integrins in the same cell, though within different lipid microdomains, via distinct Gαi protein–associated mechanisms (Shamri et al. 2002). Rapid activation of multiple integrins by a single chemokine at several cell-surface microdomains may be beneficial in triggering robust lymphocyte adhesion in the presence of continuous blood flow *in vivo*. This study also revealed that CXCL13 may contribute to a selective recruitment of circulating T cells expressing CXCR5 into LNs. Although a great majority of T cells do not express CXCR5, a small fraction of activated or memory T cells (follicular helper T cells) express this receptor (Schaerli et al. 2000, Moser et al. 2003). CXCL13 expressed in HEVs may induce trafficking of such T cells into LNs so they can interact with B cells within the secondary lymphoid tissues. This may also be true for human tonsils, where CXCL13 is expressed by a fraction of the HEVs (Schaerli et al. 2000). In summary, it was shown that CXCL13 expressed in a substantial portion of HEVs in both the LNs and PPs plays a role of an arrest chemokine for B cells. The results also suggest that CXCL13 may be a target for

the regulation of B-cell trafficking to secondary lymphoid tissues, such as LNs and PPs, and possibly to tertiary lymphoid tissues that have HEV-like venules, often found in immunological diseases such as rheumatoid synovia and atopic skin. Based on these results, several strategies for developing chemokine-directed therapeutics emerge. For example, using their functions as arrest chemokines for T cell, B cell, and monocyte homing, blocking chemokine signaling may relieve pathophysiological hyper-immune responses in many diseases. In addition, chemokine involvement in immune cell homing could be utilized to enhance immune cell recruitment to sites of infection or to other sites of tissue pathology. Recent research has shown that CXCL13 is involved in creation of anti-tumor microenvironment in subjects with high-grade serous ovarian cancer (HGSC) (Yang et al. 2021). CXCL13 shows anti-tumor activity by attracting anti-tumor $CXCR5^{+}CD8^{+}$ T cells to ovarian cancer cells, where the T cells are activated to attack the tumor. This means, in addition to its physiological function in B cell homing, CXCL13 has anti-tumor function by inducing migration of anti-tumor immune cells. Immunotherapy of tumors is an area of active research and promise. Immune checkpoint blockade therapy has been effective for a wide variety of cancers, including HGSC in human (Hamanishi et al. 2007, Disis et al. 2019). For example, Yang demonstrated that a combination of CXCL13 subcutaneous

treatment and anti-PD-1 antibody showed better efficacy than anti-PD-1 antibody monotherapy in a subcutaneous ovarian cancer mouse model. Accordingly, development of CXCL13-targeted therapy such as a recombinant CXCL13 protein, CXCL13 gene therapy, and CXCR5 agonists for certain tumors appears warranted.

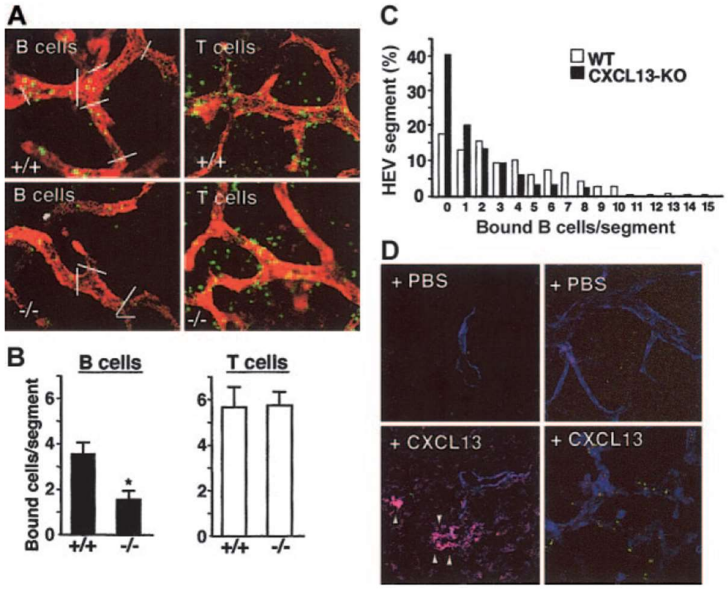

Figure 1-1. B-cell adhesion to MLN HEVs is impaired in CXCL13-deficient mice and restored by CXCL13 expression. (Kanemitsu et al. 2005)

(A) Whole-mount microscopy of MLNs from CXCL13-/- and WT mice. GFP-transgenic B or T cells (green) were injected intravenously into WT and CXCL13-/- mice. Subsequently, Alexa Fluor 594-conjugated MECA89 mAb (red) was injected to label the HEVs in situ. (B) B- and T-cell adhesion to CXCL13-/- and WT MLN HEV segments. HEVs were divided into segments as shown in (A), and the number of cells bound to each segment was determined. In each experiment, 80 HEV segments/mouse were examined. Data represent the mean ± S.D. of the number of bound cells per HEV segment in three mice. Note that the B-cell adhesion to CXCL13-/- MLN HEVs was ~40% of that seen to WT MLN HEVs (*, $P < 0.01$). (C) The frequency distribution of adherent B cells per HEV segment. (D) Restoring CXCL13 to the MLN HEVs of CXCL13-/- mice restored B-cell adhesion. After superfusion of MLNs with PBS or CXCL13, GFP-transgenic B cells and Alexa Fluor 647-conjugated MECA89 mAbs (blue) were injected and analyzed as in (A) (right panels). Frozen sections of the MLNs of these mice were stained with an anti-CXCL13 Ab (red) (left panels, arrow heads).

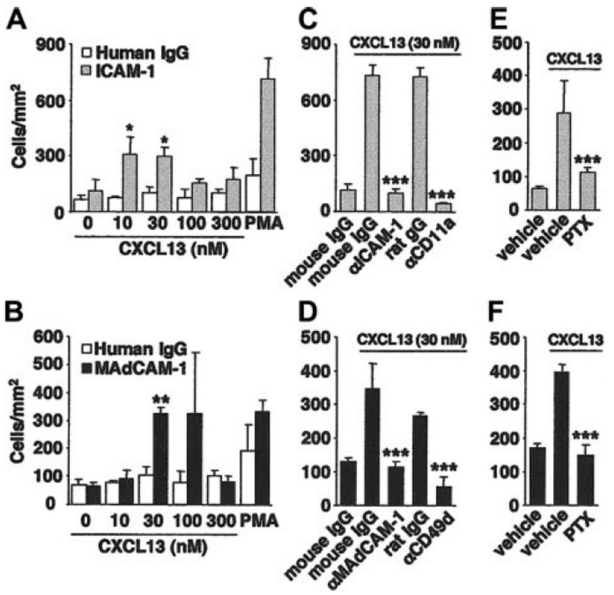

Figure 1-2. CXCL13 induces B-cell adhesion to ICAM-1 and MAdCAM-1 under static conditions. (Kanemitsu et al. 2005)

B cells were stimulated with CXCL13 and allowed to bind to immobilized ICAM-1 (A, C, and E), MAdCAM-1 (B, D, and F), or control IgG. PMA was used as a positive control. After the unbound B cells were washed off, the bound B cells were counted. The binding of B cells to ICAM-1 (A) was abrogated by mAbs to ICAM-1 or CD11a (C) or by PTX (E). Similarly, the CXCL13-induced B-cell binding to MAdCAM-1 (B) was inhibited by mAbs to CD49d or MAdCAM-1 (D) or by PTX (F). Data represent the mean ± S.D. of the number of bound B cells in triplicate fields. *, $P < 0.05$, compared with untreated B cells. **, $P < 0.01$, compared with untreated B cells. ***, $P < 0.01$, compared with control IgG- or vehicle-treated B cells.

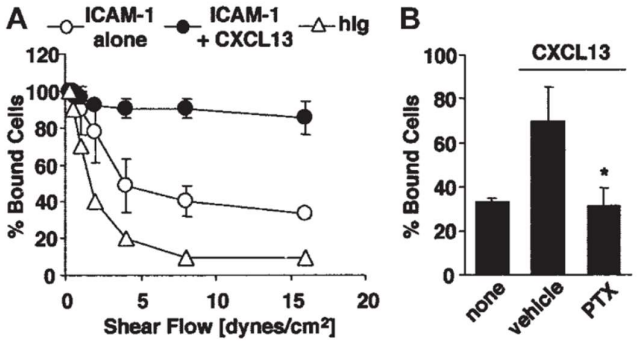

Figure 1-3. CXCL13 induces shear-resistant B-cell adhesion to ICAM-1 under flow conditions. (Kanemitsu et al. 2005)

(A) Shear-resistant B-cell adhesion to ICAM-1 alone or to ICAM-1 with CXCL13. The number of B cells that remained adherent at each shear-stress level was counted and expressed as a percentage of the initially bound B cells. (B) Pretreatment of B cells with PTX. The shear-resistant B-cell adhesion induced by CXCL13 (16 dyne/cm^2) was abrogated by PTX. Data represent the mean ± S.D. of three independent experiments. *, $P < 0.01$, compared with vehicle-treated B cells.

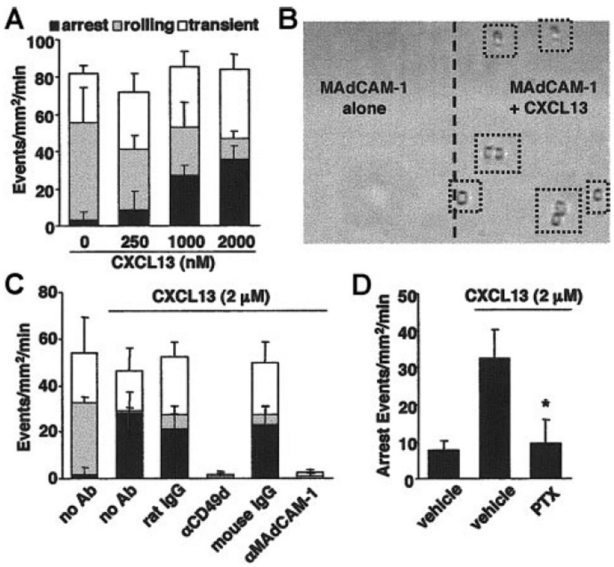

Figure 1-4. CXCL13 induces B-cell arrest on MAdCAM-1 under flow conditions. (Kanemitsu et al. 2005)

(A) B cells were injected at 1 dyne/cm^2 into capillary tubes coated with MAdCAM-1 with or without various concentrations of CXCL13. The B-cell interactions with MAdCAM-1 were classified into three categories as described in Materials and Methods. (B) B-cell arrest (dotted squares) was seen only in the CXCL13 co-immobilized area. (C) The adhesive interaction of B cells with MAdCAM-1 was abrogated by mAbs to CD49d or MAdCAM-1. (D) The CXCL13-induced B-cell arrest was inhibited by pretreatment of the B cells with PTX. Data represent the mean ± S.D. for three separate experiments. *, $P < 0.05$, compared with vehicle-treated B cells.

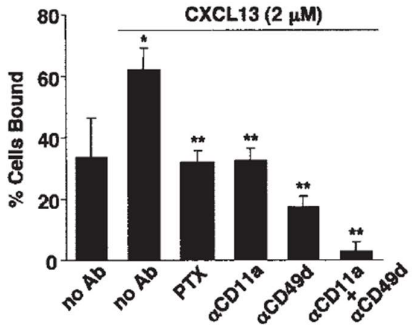

Figure 1-5. CXCL13 induces integrin-dependent B-cell adhesion to BC1 endothelial cells. (Kanemitsu et al. 2005)

B cells were perfused at 0.1 dyne/cm^2 on BC1-cell monolayers that were untreated or had been treated with CXCL13. Shear stress was applied at 2 dyne/cm^2 for 10 min and the number of remaining adherent B cells was counted. Results are expressed as the percentage of input cells remaining bound. For inhibition studies, B cells were treated with PTX or mAbs to CD11a or CD49d. Data represent the mean ± S.D. for three separate experiments. *, $P < 0.01$, compared with untreated BC1 cells. ** $P < 0.01$, compared with vehicle- or control IgG-treated B cells.

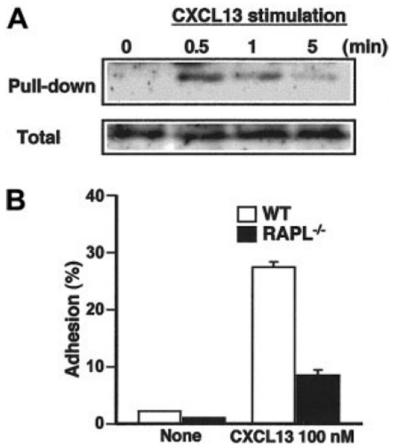

Figure 1-6. CXCL13 activates signal transduction pathways involving Rap1 and RapL. (Kanemitsu et al. 2005)

(A) Activation of Rap1 in CXCL13-stimulated B cells. B cells were stimulated with CXCL13 (30 nM) for the indicated times and subjected to a pull-down assay with Ral GDS-RBD. The amounts of GTP-Rap1 (upper) and total Rap1 protein (lower) were examined by western blotting with an anti-Rap1 antibody. (B) Shear-resistant adhesion of wild-type (WT) and RapL-deficient B cells to ICAM-1. Cells were stimulated with CXCL13 (100 nM) and allowed to bind ICAM-1. Shear-resistant B-cell adhesion (2 dyne/cm^2) was examined by parallel flow chamber assay.

Chapter 2: Chronic treatment with the (iso-)glutaminyl cyclase inhibitor PQ529 is a novel and effective approach for glomerulonephritis in chronic kidney disease

Introduction

Chronic kidney disease (CKD) results in long-term kidney dysfunction. CKD is relatively prevalent, with over 10% of the adult population in developed countries estimated to suffer from the disease (Lopez-Novoa et al. 2010). CKD occurs when strain is placed on the kidneys, e.g., by combinations of problems such as high blood pressure, diabetes, high cholesterol, kidney infection, and glomerulonephritis. A decrease of renal function is considered an independent risk factor for both cardiovascular diseases and mortality in the general population.

A cure for CKD remains elusive. Although many treatments have been developed for CKD, including angiotensin-converting enzyme (ACE) inhibitors and angiotensin receptor blockers (ARBs), the absolute risk of morbidity and mortality of renal and cardiovascular dysfunctions in CKD patients remains high (Lambers Heerspink and de Zeeuw 2013). Novel CKD treatments are needed, either

singly or in combination with existing therapies.

CCL2 (C-C motif Ligand 2, MCP-1) is a chemokine of the CC chemokine subfamily. CCL2 has chemo-attractive activity for several types of immune cells, including monocytes and macrophages, that express its corresponding receptor, CCR2 (C-C chemokine receptor type 2, CD192), on their cell surface. Migration of these immune cells to sites of inflammation is induced by binding of CCL2 to CCR2 (Carr et al. 1994, Xu et al. 1996, Gschwandtner et al. 2019). Macrophage signal transduction through the CCL2/CCR2 axis reportedly causes injury in the nephrons and renal tubes of CKD patients, which can lead to glomerulonephritis and diabetic kidney diseases (Wada et al. 2000, Tesch et al. 1999, Giunti et al. 2010, Tampe et al. 2014, Haller et al. 2016, Moreno et al. 2018). In these diseases, overexpression of CCL2 increases homing of macrophages to the tubulointerstitium and glomerulus (Viedt et al. 2002), resulting in glomerulonephritis and proteinuria (Banba et al. 2000, Eardley et al. 2006).

The effects of inhibition of the CCL2/CCR2 axis on CKD have been demonstrated in several animal models (Lloyd et al. 1997, Kitagawa et al. 2004, Kang et al. 2010, Sayyed et al. 2011). Inhibitors for CCL2/CCR2 axis, such as

CCX140-B and emapticap pegol, are of clinical benefit for diabetic kidney disease patients (DeZeeuw et al. 2015, Menne et al. 2017). Therefore, it has been suggested that inhibition of the CCL2/CCR2 axis would be a clinically meaningful approach to manage CKD.

The biological activity of CCL2 is stabilized by pyroglutamylation (pE-) at its N-terminus, formation of which is catalyzed by glutaminyl cyclase (QC) and isoQC (Cynis et al. 2008). When QC/isoQC inhibitors block pyroglutamylation, CCL2 becomes structurally unstable, leading to loss of activity and increased degradation (Cynis et al. 2011, Ling and Luster 2011, Chen YL et al. 2012). Given this evidence, it was hypothesized that inhibition of QC/isoQC activity would be of benefit in CKD. This hypothesis has been tested, using a rat model of glomerulonephritis, by treating the animals with PQ529, a QC/isoQC inhibitor. The potential of CCL2 levels was also evaluated in urine and blood as disease biomarkers (Morgan et al. 2012) and as a measure of the effectiveness of QC/isoQC inhibitors.

Materials and Methods

QC/isoQC inhibitor

A QC/isoQC inhibitor was synthesized and used as described in Kanemitsu et al. 2021. 1-(1*H*-Benzimidazol-6-yl)-5-(4-propoxyphenyl)imidazolidine-2,4-dione (PQ529; Probiodrug, Halle, Germany) [Cynis H. 2011] was synthesized at Astellas Pharma Inc. (Ibaraki, Japan).

Ethics statement

Animals used in this study and their handling conditions are described in Kanemitsu et al. 2021. Animals were housed under controlled temperature, humidity, and light (12-h light-dark cycle) conditions and provided a standard commercial diet and water *ad libitum*. Animals were handled in accordance with the *Guide for the Care and Use of Laboratory Animals*, and all procedures were approved by the Animal Ethics Committee of Astellas Pharma Inc.

Pharmacokinetics

Pharmacokinetics assay was conducted as described in Kanemitsu et al. 2021. After oral administration of PQ529 (30 and 100 mg/kg) to non-fasting male

Wistar rats, blood (0.2 mL) was drawn via jugular vein cannulation after 0.5, 1, 2, 4, and 6 h and then centrifuged to obtain the plasma fraction. The test compound in plasma samples was extracted by deproteination with acetonitrile and then analyzed by liquid chromatography-tandem mass spectrometry (LC-MS/MS).

Antibody to rat pE-CCL2

An antibody to rat pE-CCL2 was synthesized and used as described in Kanemitsu et al. 2021. Genes of anti-rat pE-CCL2 antibody heavy chain and anti-rat pE-CCL2 antibody light chain (Kanemitsu et al. 2021) were synthesized (Life Technologies Japan, Tokyo, Japan) and sub-cloned into pEE6.4 vector and pEE12.4 vector (The GS Gene Expression System™; Lonza, Basel, Switzerland), respectively. Both vectors (0.3 mg for each) were mixed and incubated with 1.2 mL of 293fectin™ Transfection Reagent (Thermo Fisher Scientific, Waltham, MA, USA) in 20 mL of OPTIMEM (Thermo Fisher Scientific) at room temperature (RT) for 30 min. They were then applied to FreeStyleTM 293-F cells (Thermo Fisher Scientific) followed by incubation at 37°C in 8% CO_2 for 5 days. The supernatant of the Freestyle 293-F cells was collected and then applied to Protein G Sepharose 4 Fast Flow antibody purification resin (GE Healthcare, Chicago, IL, USA) to

purify anti-pE-CCL2 antibody.

Pharmacodynamics

Pharmacodynamics assay was conducted as described in Kanemitsu et al. 2021. Ten minutes after oral administration of PQ529 (30 and 100 mg/kg) to non-fasting male Wistar rats, lipopolysaccharide (LPS; from *Escherichia coli* 055:B5, 0.5 mg/kg, 3,000,000 endotoxin units/mg; Sigma-Aldrich, St. Louis, MO, USA) was injected intraperitoneally. Blood was drawn from the abdominal vena cava using a 19- to 23-gauge needle under isoflurane anesthesia at 0 (pre-PQ529 treatment), 1, 2, 3, and 5 h and then centrifuged at ≅15,000 *g* to produce plasma from which the levels of pE-CCL2 were determined. Heparin was used as the anti-coagulation reagent. Plasma pE-CCL2 levels were measured by enzyme-linked immunosorbent assay (ELISA). Anti-rat pE-CCL2 antibody binding to ELISA plates (White 384-Well MaxiSorp^{TM} Plates; Thermo Fisher Scientific) was performed in phosphate-buffered saline (PBS) at 4°C overnight, followed by blocking with 4% BSA and 0.1% (v/v) Tween 20 in PBS at room temperature for 30 minutes. After washing 3 times with 0.1% Tween 20 in PBS, plasma samples or standard rat CCL2 (PeproTech, Rocky Hill, NJ, USA) were added and incubated for 2 h at RT, followed by three additional washes. Biotin-conjugated anti-pE-

CCL2 antibody diluted in Can Get Signal Solution 1 (TOYOBO, Osaka, Japan) was added and incubated for 2 h at RT, followed by washing. Avidin-conjugated HRP (Thermo Fisher Scientific) diluted in Can Get Signal Solution 2 (TOYOBO) was then added and incubated for 1 to 1.5 h at RT, followed by washing. Finally, SuperSignal™ ELISA Femto Substrate (Thermo Fisher Scientific) was added, and the signal intensity and background of each well was measured and recorded with Envision (PerkinElmer, Waltham, MA, USA).

Rat model of anti-glomerular basement membrane glomerulonephritis

CKD model rats were prepared, and treatment of PQ529 in the model rats was conducted as described in Kanemitsu et al. 2021. Rabbit anti-glomerular basement membrane serum (IBL, Fujioka, Japan) was intravenously administered to 6-week-old male WKY rats (N = 30) (Charles River Laboratories Japan, Inc., Kanagawa, Japan). Age-matched rats were used as normal controls (N = 10). Spontaneously voided urine was collected for 24 h from animals in metabolic cages, and blood samples were taken at weeks 0 (a day before anti-GBM serum injection), 1, 2, and 3. Urinary protein concentrations were measured using a protein assay reagent (Bio-Rad Laboratories, Inc., Hercules, CA, USA). Plasma and urine creatinine and blood urea nitrogen (BUN) levels were measured using a Hitachi

7180 automatic analyzer (Hitachi High-Technologies Corporation, Tokyo, Japan). Total CCL2 in serum and urine were measured using an ELISA kit (DAKO, Inc., Carpinteria, CA, USA). Urine KIM-1, β2 microglobulin, and clusterin were measured using WideScreen^{TM} Rat Kidney Toxicity Panel 1 and 2 (Merck, Kenilworth, NJ, USA).

Anti-GBM serum-injected rats were grouped such that urinary protein excretion, plasma creatinine and BUN levels, urine volume, and body weight were uniform among the groups. Group compositions were as follows: (1) normal rats (N = 10), anti-GBM serum injected rats treated with (2) vehicle (N = 10), (3) PQ529 (30 mg/kg, N = 10), and (4) PQ529 (100 mg/kg, N = 10). PQ529 was orally administered to the rats twice a day for 3 weeks. At weeks 0, 1, 2, and 3, the serum CCL2 and creatinine, BUN, 24-h urinary protein excretion, urine creatinine, KIM-1, β2 microglobulin, and clusterin levels were measured. After 24-h urinary collection at week 3, blood samples were collected from the abdominal vena cava under isoflurane anesthesia, and one kidney was removed from each rat and

weighed.

Sample processing

Sample processing was conducted as described in Kanemitsu et al. 2021. Urine samples collected over 24 h in metabolic cages were centrifuged at 3000–6000 *g* and then urinary protein, creatinine, CCL-2, KIM-1, clusterin, and β2 microglobulin were measured in the resulting plasma. Blood samples were collected under isoflurane anesthesia from the retro-orbital venous plexus (at weeks 0, 1, and 2) using heparin-coated glass capillaries (Terumo Corporation, Tokyo, Japan) or from the abdominal vena cava (at week 3) using 19- to 23-gauge needles. The blood was centrifuged at ≅15,000 *g* to measure the levels of serum or plasma creatinine, CCL2, and BUN in the supernatant. Heparin was used as the anti-coagulation reagent.

Kidneys removed from the animals were weighed and sectioned in halves in the transverse plane. The upper half of one of the organs was immersed in 10% neutral-buffered formalin for histological evaluation and the cortex of the remaining half was frozen in liquid nitrogen and stored at -80°C until processing for mRNA quantification. The other kidney was lysed with Pierce™ IP Lysis Buffer

(Thermo Fischer Scientific) containing 1x of Halt™ Protease Inhibitor Cocktail, EDTA-free (Thermo Fischer Scientific) to measure kidney CCL2 using an ELISA Kit (DAKO, Inc.) and kidney IFN-γ using a rat IFN-gamma Quantikine ELISA Kit (R&D systems, Minneapolis, MN, USA).

Quantification of renal RNA

Renal RNA was quantified as described in Kanemitsu et al. 2021. Total renal RNA was extracted using an RNeasy Mini Kit (QIAGEN, Hilden, Germany) in accordance with the manufacturer's instructions. Complementary DNA was synthesized using a SuperScript™ VILO™ cDNA Synthesis Kit (Thermo Fischer Scientific). Real-time polymerase chain reaction (PCR) was used to quantify the CD68 and CCL2 gene expression with the following primers: 5'-GAACCCGAACAAAACCAAGGT-3' and 5'-AGCTGTCCGTAAGGGAATGAGA-3' for CD68 and 5'-CAGCACCTTTGAATGTGAACTTG-3' and 5'-TGCTTGAGGTGGTTGTGGAA-3' for CCL2. Reactions were performed using SYBR Green with an ABI PRISM 7900 Sequence Detection System (Applied Biosystems, Foster City, CA, USA). Data were normalized to endogenous hypoxanthine-guanine phosphoribosyltransferase (HPRT) or to a β-actin mRNA

control.

Histology

Histological assay was conducted as described in Kanemitsu et al. 2021. Specimen preparation and histopathological examinations were performed at the Drug Safety Research Laboratories of Astellas Pharma Inc. Renal tissues fixed in 10% neutral-buffered formalin were embedded in paraffin, sectioned at 3 μm, and stained with hematoxylin and eosin (H&E) and periodic acid-Schiff (PAS). Mononuclear cell infiltration into kidney was quantified as previously described (Huan Y et al, 2014). The total number of interstitial cell clusters, the size of each cluster, and the total cumulative size of the clusters in randomly selected, non-overlapping, 10 visual fields per H&E-stained kidney section was determined using Aperio ImageScope version 12.3.3.5048 image analysis software (Leica Biosystems, Wetzlar, Germany). To determine the degree of glomerulosclerosis, a semiquantitative score was obtained from PAS-stained sections by grading segmental and global sclerosis (grade 0: no damage, 1: segmental sclerosis in <50%, 2: segmental sclerosis in ≥50%, 3: global sclerosis in <25%, 4: global sclerosis in ≥25% of the glomeruli in the visual field). To determine the degree of tubulointerstitial damage, a semi-quantitative score was obtained from H&E-

stained sections by grading dilation of the renal tubules, thickening of the basement membrane, urinary cast, basophilic changes in the tubular epithelium, and hyaline droplet deposition (grade 0: no damage, 1: damage in 25%, 2: damage in half, 3: damage in 75%, 4: damage in the whole area of the renal cortex in the visual field).

Statistical analyses

Statistical analyses were conducted as described in Kanemitsu et al. 2021. Results are expressed as the mean ± standard deviation (S.D.). Significance was determined using Student's *t*-test, while those among multiple groups were assessed using a one-way analysis of variance followed by Dunnett's multiple comparisons test as a post hoc test. Correlations were analyzed using Pearson's rank correlation. Histopathological scores were compared using a Mann-Whitney test to analyze differences between two groups, while a nonparametric Kruskal-Wallis analysis of variance followed by Dunn's multiple comparisons test was used for comparisons among multiple groups. A value of $p < 0.05$ was considered significant. Statistical and data analyses were conducted using GraphPad Prism 8.0.2 (GraphPad Software, San Diego, CA, USA).

Results

Pharmacokinetic and pharmacodynamic profiles of PQ529

After oral dosing of PQ529 (30 and 100 mg/kg) to Wistar rats, the plasma concentration of free, unmodified Q529 peaked at 30 minutes (6.5 and 33 μM of plasma concentrations at 30 and 100 mg/kg of the compound, respectively) and then gradually decreased (Fig. 2-1a), with a terminal half-life of 0.5–1.0 hours. Using an estimate for free, unmodified PQ529 of 12% (unpublished data), we found that concentrations of PQ529 in the blood of animals 30 min after dosing with 30 or 100 mg/kg of the compound were ~784 and ~4000 nM, respectively.

The IC_{50} of the blocking effects of PQ529 on human, murine, and rat isoQC enzymatic activity were 37, 43, and 20 nM, respectively. Additionally, the IC_{50} for effects of PQ529 on the QC/isoQC in mouse Raw264.7 and human THP-1 cells were 630 and 1500 nM, respectively (data not shown). In our pharmacodynamics study, doses of 30 or 100 mg/kg of PQ529 inhibited LPS-induced pE-CCL2 production by ~30% and ~50%, respectively, as measured 2 h after the LPS injection (0.5 mg/kg) (Fig. 2-1b).

Effects of repeated dosing of PQ529 on kidney function and plasma, urine, and kidney CCL2 levels in a rat model of glomerulonephritis

No deaths were observed in any tested rats during the drug administration period. Compared with normal rats, anti-GBM-induced glomerulonephritis led to progressive increases in urinary protein excretion and BUN. Repeated administration of PQ529 (30 and 100 mg/kg) attenuated the increase of urinary protein and BUN in a dose-dependent manner at week 3 (Fig. 2-1c and Table 2-1). Additionally, the concentration of total CCL2 in serum and urine was significantly elevated in the glomerulonephritis rats past two weeks following the anti-GBM serum injection. At necropsy, expression of CCL2 in kidney was significantly higher in the glomerulonephritis rats compared to the normal rats. Repeated administration of PQ529 significantly inhibited the increase of CCL2 levels in serum, urine, and kidney in a dose-dependent manner (Fig. 2-2a, b, and c) after 3 weeks of PQ529 treatment. Urinary protein excretion and CCL2 levels in serum ($r = 0.87$, 95% confidence interval [CI] = 0.76-0.93, $p < 0.01$), urine ($r = 0.76$, 95% CI = 0.59-0.87, $p < 0.01$), and kidney ($r = 0.91$, 95% CI = 0.84-0.95, $p < 0.01$) were positively correlated (Fig. 2-2d, e, and f).

Effects of repeated dosing of PQ529 on mononuclear cell infiltration into kidney, glomerulosclerosis, and tubulointerstitial injury in glomerulonephritis rats

In the glomerulonephritis rats at necropsy, mRNA levels of CD68 and CCL2 in the kidney cortex were increased significantly. Repeated administration of PQ529 resulted in significant suppression of increased CD68 and CCL2 mRNA levels in a dose-dependent manner (Fig. 2-3a and b). Histological analyses of the kidneys of tested animals showed an increase in mononuclear infiltration into the interstitium in the glomerulonephritis rats and suppression of the infiltration by the repeated dosing of PQ529 (Fig. 2-4a, b, and c). Additionally, PQ529, at 100 mg/kg, decreased the severity of glomerulosclerosis and tubulointerstitial injury (Fig. 2-5a and 5b).

Kidney injury molecule-1 (KIM-1), β2 microglobulin, and clusterin levels in the urine, as well as IFN-γ expression in the kidney cortex, progressively increased in the glomerulonephritis model rats relative to the normal rats. Repeated dosing of PQ529 lowered the levels of KIM-1, β2 microglobulin, clusterin, and IFN-γ expression in the kidneys in a dose dependent manner (Fig. 2-6a, b, c, and d). These effects were statistically significant at 100 mg/kg.

Discussion

It is known that a final common pathway in CKD shows a correlation between macrophage infiltration and fibrosis in kidney (Hodgkins et al. 2012 and Yonemoto et al. 2006). CCL2/CCR2 signaling induces mononuclear cell infiltration and inflammation in the kidney (Tesch et al 1999, Giunti et al. 2010, Tampe et al. 2014, Haller et al. 2016, Moreno et al. 2018), and inhibition of this signal pathway shows beneficial effects in CKD animal models (Lloyd et al. 1997, Kitagawa et al. 2004, Kang et al. 2010, Sayyed et al. 2011) and in humans (DeZeeuw et al. 2015, Perez-Gomez et al. 2016, Menne et al. 2017). Furthermore, some reports show that the urinary CCL2 levels correlate with urinary protein levels (Banba et al. 2000, Eardley et al. 2006), so urinary CCL2 level may be used as a biomarker for CKD (Verhave et al. 2013, Siddiqui et al. 2019). Genetic variants of CCL2 (e.g., an A/G polymorphism at nucleotide position 2518 in the distal 5' regulatory region) reportedly also correlates with the risk of IgA nephropathy in humans (Gao et al. 2016). Here, I showed that administration of the QC/isoQC inhibitor PQ529 protected the kidneys of anti-GBM serum-induced glomerulonephritis rats from progressive dysfunction. Inhibition of CCL2/CCR2 signal transduction thus may be a novel, effective approach for the treatment of CKD.

The anti-GBM serum-induced glomerulonephritis rat model of CKD often is used to investigate the disease mechanism and evaluate novel treatments for CKD. In this CKD model, expression of CCL2 increases in the tubulointerstitium and glomeruli immediately after administration of the anti-GBM serum (Tang 1996, Natori 1997). Increased kidney CCL2 levels in this model also appear to be involved in the progression of kidney dysfunction, as evidence by tubulointerstitial fibrosis, glomerulonephritis, and massive proteinuria accompanied by monocyte and macrophage migration to the kidneys (Taniguchi 2007). Blockage of CCL2/CCR2 signaling by anti-CCL2 antibodies and CCR2 inhibitors attenuates proteinuria and inflammation in the tubulointerstitium and glomeruli and suppresses mononuclear cell infiltration (Wada et al. 1996). In the present study, repeated administration of PQ529 significantly decreased CCL2 levels systemically (in serum and urine) and locally (in the kidney itself), suggesting that inhibition of QC/isoQC decreases the levels of stable, pE-modified CCL2 *in vivo*. Several articles have shown that the CCL2/CCR2 axis is involved in the final common pathway of CKD and that inhibitors of this axis were effective in CKD animal models (Kang et al. 2010, Sayyed et al. 2011). Development of more potent QC/isoQC inhibitors may lead to increased inhibition of the CCL2/CCR2 axis in the glomerulonephritis model. Taken together, these reports suggest that inhibitors

of QC/isoQC are effective against not only glomerulonephritis but also kidney inflammation in CKD.

In this study, CCL2 level was determined by using a commercial ELISA kit. This method detects epitopes other than pE-N-terminal amino acids, meaning that the levels of CCL2 in the *in vivo* model represent total CCL2 levels. This method was used in the glomerulonephritis rat studies because pE-CCL2 levels were below the limit of detection, whereas pE-CCL2 levels were easily determined in the rat PD model using LPS as stimulator of CCL2 production. Nevertheless, regardless of CCL2 detection method, decreases in total CCL2 levels after continuous treatment with PQ529 show that this compound is an effective inhibitor of the CCL2/CCR2 axis.

Sayyed et al. have shown that CCL2 in blood induces the migration of CCR2-expressing monocytes through the bone marrow into the blood stream and that CCL2 in the tubulointerstitium induces macrophage infiltration to sites of inflammation in CKD kidneys (Sayyed et al. 2011). I observed decreased serum CCL2 levels, but macrophage concentrations in the blood were not determined, something that should be done in the future. It was also found that decreases in

CCL2 protein in the kidney positively relate to mononuclear cell infiltration. However, the decrease in expression of CD68 in the kidney was less than the semiquantitative scores of mononuclear cell infiltration. Because the histopathological data are evaluated semi-quantitatively, comparison between the effect of PQ529 on CD68 expression and its effect on of mononuclear cell infiltration may not be appropriate. Determining the time course of macrophage infiltration by immunohistochemical methods would be a better approach to explain differences of effects of the treatment on CCL2 protein, CD68 expression, and monocyte infiltration in the kidney.

The decrease in CCL2 mRNA expression in PQ529-treated glomerulonephritis rats may have been caused by a decrease in inflammation in the tubulointerstitium as a result of reduced macrophage infiltration. The following observations were also noted: reductions in the levels of the tubular injury markers KIM-1, β2 microglobulin, and clusterin in urine; decreased IFN-γ expression in the kidney; and reduced tubulointerstitial injury in these animals. A trend towards decreased glomerulosclerosis of the kidneys of PQ529-treated rats was seen. Collectively, these data suggest that PQ529-induced reductions of mononuclear cell or macrophage infiltration of the kidney prevent kidney injury, although it is

difficult to confirm this because of the semiquantitative nature of histopathological analyses. In addition, other chemokines and a cytokine (CCL5 [RANTES], CXCL8 [IL-8], or PDGF) have been reported to contribute to glomerulonephritis (Stasikowska et al. 2007). Further studies will be needed to elucidate the roles of these different cytokines in CKD.

Chronic PQ529 treatment reduced proteinuria and kidney inflammation in the glomerulonephritis rats, results that support the potential benefits of inhibitors of CCL2/CCR2 signaling in CKD. Furthermore, total CCL2 levels in both serum and urine were reduced in a dose dependent manner by chronic treatment with PQ529. Recently, it has been reported that confirming pharmacological signals of administered drugs in early development is important for more efficient drug development (Morgan et al. 2012). This study shows that serum and urine CCL2 are pharmacodynamic biomarkers of QC/iso QC inhibitors for CKD, making use of these inhibitors for CKD preferable to using other CCL2/CCR2 axis inhibitors for which no proof of pharmacology biomarkers exist.

In recent years, clinical studies of inhibitors of CCL2/CCR2 signaling, such as emapticap pegol and CCX140-B, were conducted in patients with diabetic

kidney disease. Neither of the compounds had significant effects on proteinuria in these phase 2 trials, but a trend toward improvement was observed. Interestingly, lower doses (5 mg) were more effective than higher doses (10 mg), which caused higher CCL2 expression (deZeeuw et al. 2015), likely due to a compensatory response to receptor blockade by CCX140-B. It was confirmed in human THP-1 cells that CCX140-B itself increased the levels of LPS-induced pE-CCL2, whereas, in contrast, PQ529 decreased the levels (data not shown). It was also confirmed that chronic treatment with PQ529 decreased CCL2 mRNA expression in the kidneys of glomerulonephritis rats, suggesting that PQ529 does not have compensatory effects on CCL2 expression in *in vitro* or *in vivo*. These findings suggest that compensatory elevations of CCL2 in humans should not be expected due to chronic administration of QC/isoQC inhibitors. This prediction is supported by the observed decreases of serum, urine, and kidney CCL2 in glomerulonephritis rats treated with PQ529. CCL2 levels in serum and urine can serve as biomarkers of disease state and effects, which means they would be of tremendous value as efficacy measures in phase 1, 2, and 3 clinical trials.

Findings in this study suggest that CCL2/CCR2 signaling plays a crucial role in glomerulonephritis in CKD and that the QC/isoQC inhibitor PQ529 can

inhibit this signaling by blocking pyroglutamylation of the N-terminal glutamine of CCL2. These results in suppression of kidney inflammation and inhibits the progression of renal dysfunction. Chronic treatment with QC/isoQC inhibitors thus may be a novel and effective approach for treating glomerulonephritis and CKD.

Table 2-1. Effect of repeated administration of PQ529 on general parameters in glomerulonephritis rats. (Kanemitsu et al. 2021)

PQ529 was orally administered to glomerulonephritis rats twice daily for three weeks. The values are the mean ± standard deviation for 10 animals per group.

Index	Normal	Glomerulonephritis		
	Vehicle	Vehicle	30 mg/kg	100 mg/kg
Body weight (g)	265±17	252±8*	257±9	257±11
Food intake (g/day)	17.1	16.1	16.7	17.5
Creatinine clearance (mL/day/100 g body weight)	1397±98	893±131*	854±190	1041±154
Blood urea nitrogen (mg/dL)	13.2±1.5	18.0±4.6*	16.4±2.8	13.6±2.5#

*$p<0.05$ vs. normal group using Student's t test

#$p<0.05$ vs. glomerulonephritis vehicle group using Dunnett's multiple comparison test

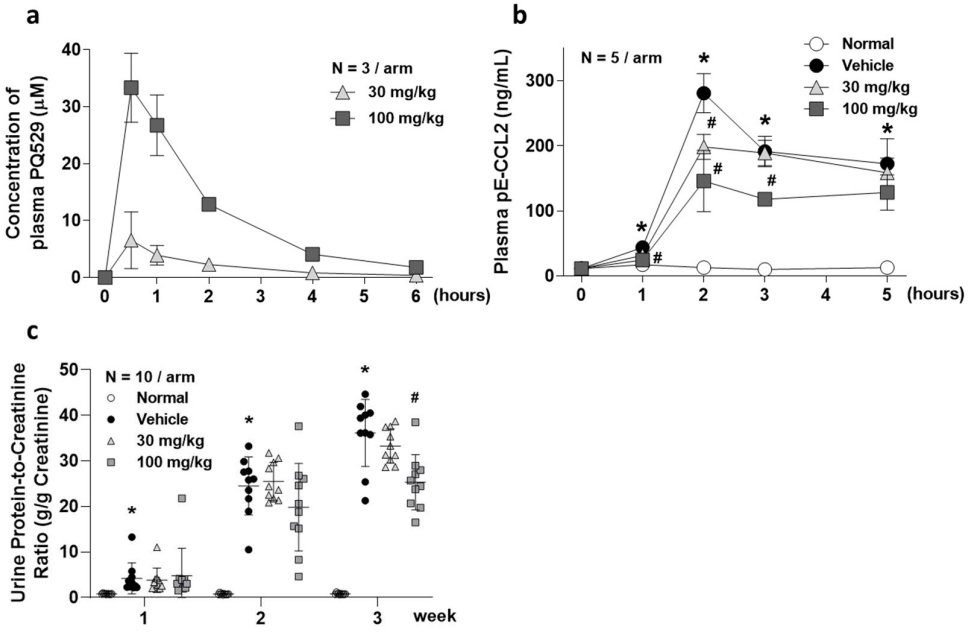

Figure 2-1. Pharmacokinetics and pharmacodynamics of PQ529 in Wistar and WKY rats and effect of repeated administration of PQ529 on the urinary protein excretion in anti-GBM-induced glomerulonephritis rats. (Kanemitsu et al. 2021)

(a) Time course of changes in the plasma concentration of the unchanged PQ529 (30 and 100 mg/kg) in male Wistar rats. (b) Time course of changes in the plasma concentration of pE-CCL2 after the administration of PQ529 (30 and 100 mg/kg) to WKY rats. (c) PQ529 was orally administered to anti-GBM-induced glomerulonephritis rats twice daily for three weeks. Data are expressed as the mean ± S.D. for (a) three Wistar rats and (b) five WKY rats per sampling point and (c) ten WKY rats per group. The results are expressed as the mean ± standard deviation (S.D.). Significant differences between two groups were assessed using Student's *t*-test, while those among multiple groups were assessed using a one-way analysis of variance followed by Dunnett's multiple comparisons test as a post hoc test. *$p<0.05$ vs. normal group, #$p<0.05$ vs. vehicle group

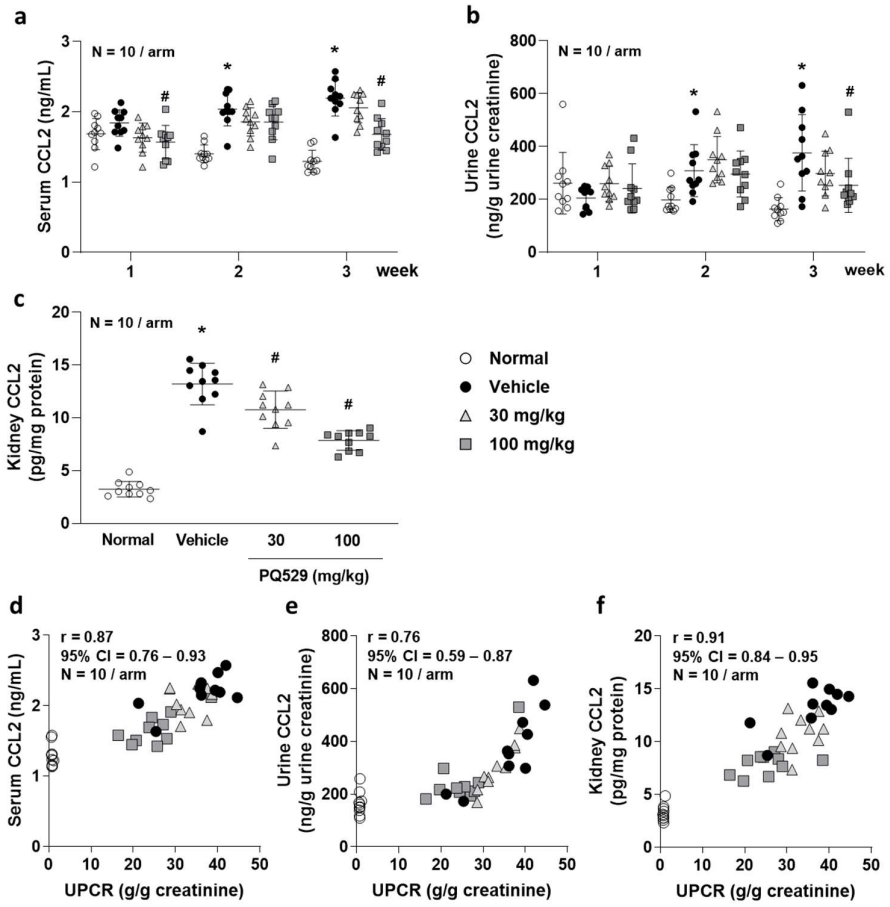

Figure 2-2. Effect of repeated administration of PQ529 on (a) serum, (b) urine, and (c) kidney CCL2 and correlation between (d) serum, (e) urine, and (f) kidney CCL2 and urine protein-to-creatinine ratio in anti-GBM-induced glomerulonephritis rats. (Kanemitsu et al. 2021)

PQ529 was orally administered to anti-GBM-induced glomerulonephritis rats twice daily for three weeks. Data are expressed as the mean ± S.D. for 10 animals per group. The results are expressed as the mean ± standard deviation (S.D.). Significant differences between two groups were assessed using Student's *t*-test, while those among multiple groups were assessed using a one-way analysis of variance followed by Dunnett's multiple comparisons test as a post hoc test. Correlations were analyzed using Pearson's rank correlation. *p<0.05 vs. normal group, #p<0.05 vs. vehicle group

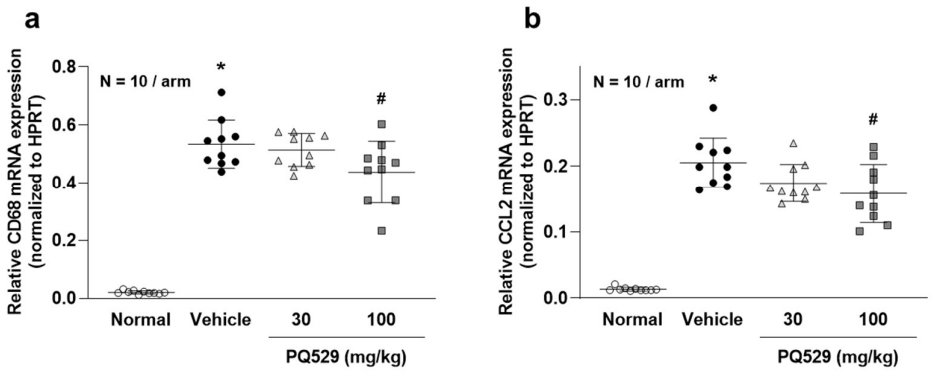

Figure 2-3. Effect of repeated administration of PQ529 on renal (a) CD68 and (b) CCL2 expression in anti-GBM-induced glomerulonephritis rats. (Kanemitsu et al. 2021)

PQ529 was orally administered to anti-GBM-induced glomerulonephritis rats twice daily for three weeks. Data are expressed as the mean ± S.D. for 10 animals per group. The results are expressed as the mean ± standard deviation (S.D.). Significant differences between two groups were assessed using Student's *t*-test, while those among multiple groups were assessed using a one-way analysis of variance followed by Dunnett's multiple comparisons test as a post hoc test. *$p<0.05$ vs. normal group, #$p<0.05$ vs. vehicle group

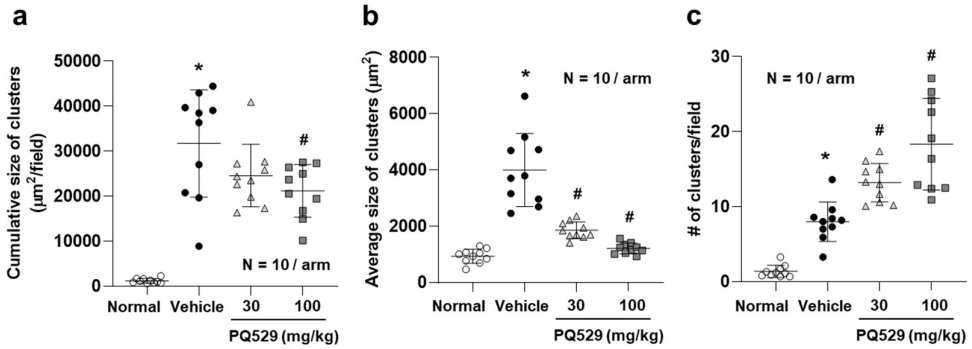

Figure 2-4. Effect of repeated administration of PQ529 on mononuclear cell infiltration in glomerulonephritis rats. (Kanemitsu et al. 2021)

PQ529 was orally administered to glomerulonephritis rats twice daily for three weeks. Data are expressed as the mean ± S.D. for 10 animals per group. Significant differences between two groups were assessed using Student's *t*-test, while those among multiple groups were assessed using a one-way analysis of variance followed by Dunnett's multiple comparisons test as a post hoc test. *$p<0.05$ vs. normal group, #$p<0.05$ vs. vehicle group.

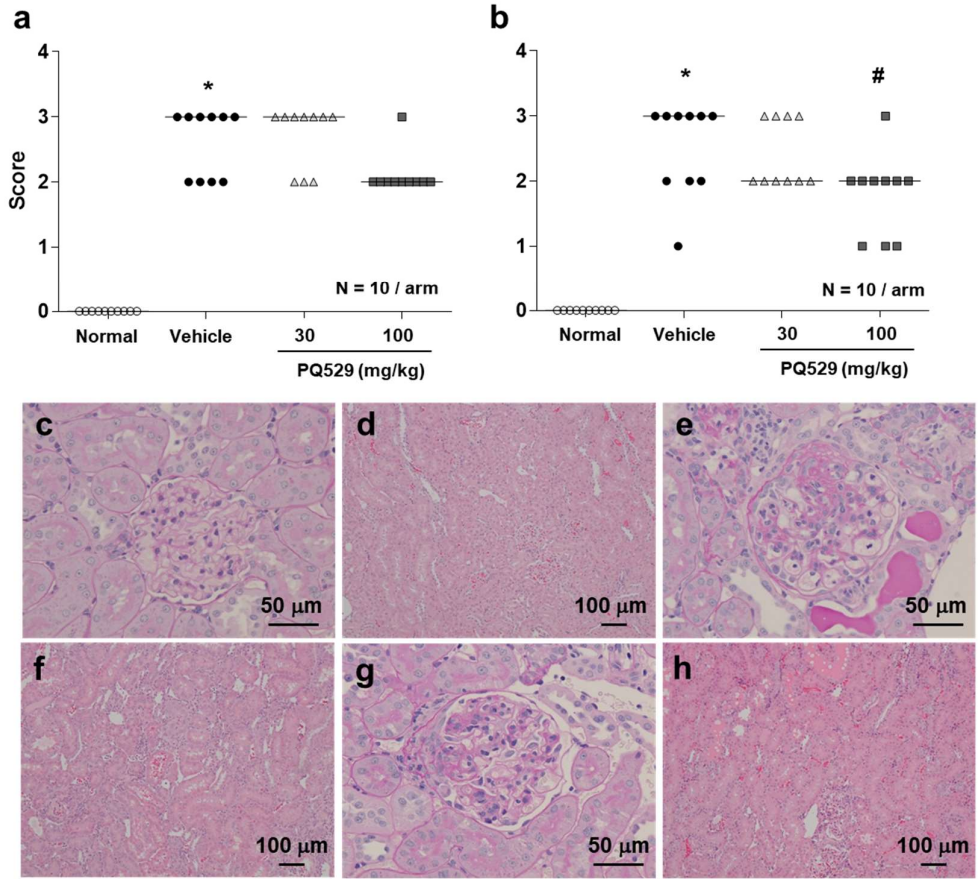

Figure 2-5. Effect of repeated administration of PQ529 on (a) glomerulosclerosis and (b) tubulointerstitial damage in glomerulonephritis rats and representative light micrographs of renal tissues obtained from (c, d) normal (semiquantitative scores of glomerulosclerosis, tubulointerstitial damage: 0, 0), (e, f) glomerulonephritis (scores: 3, 3), and (g, h) PQ529 (100 mg/kg)-treated rats (scores: 2, 1). (Kanemitsu et al. 2021)

Magnification: left, ×40 (PAS stain); right, ×10 (H&E stain). PQ529 was orally administered to glomerulonephritis rats twice daily for three weeks. Data are expressed as the median for 10 animals per group. Histopathological non-parametric scores were compared using a Mann-Whitney test to analyze differences between two groups, while a nonparametric Kruskal-Wallis analysis of variance followed by Dunn's multiple comparisons test was used for comparisons among multiple groups. *$p<0.05$ vs. normal group, #$p<0.05$ vs. vehicle group.

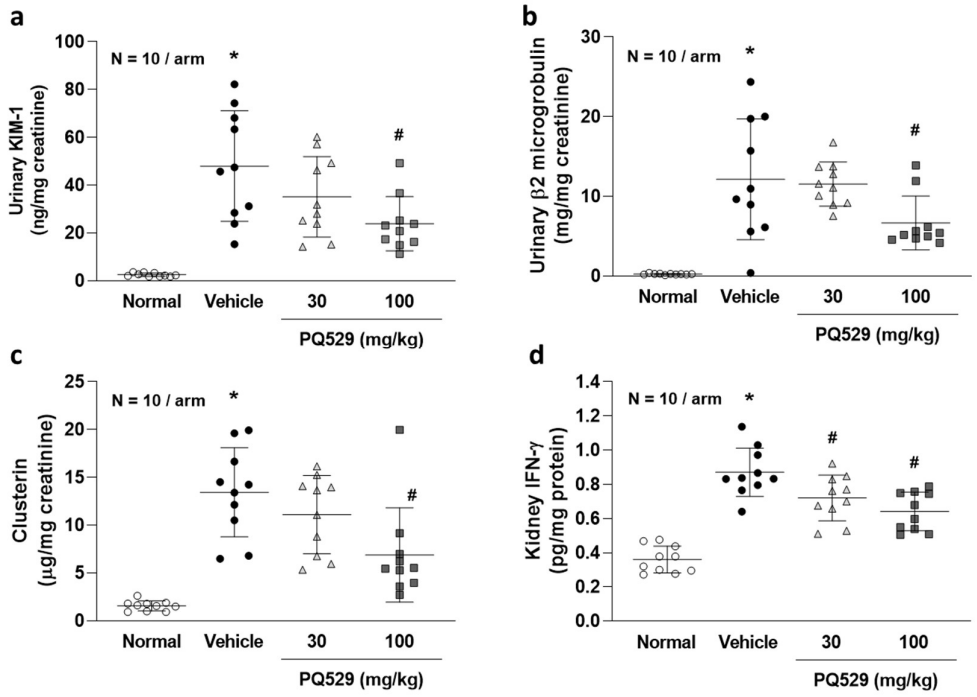

Figure 2-6. Effect of repeated administration of PQ529 on the urinary (a) KIM-1, (b) β2 microglobulin, and (c) clusterin levels and (d) kidney IFN-γ levels in anti-GBM-induced glomerulonephritis rats. (Kanemitsu et al. 2021)

PQ529 was orally administered to anti-GBM-induced glomerulonephritis rats twice daily for three weeks. Data are expressed as the mean ± S.D. for 10 animals per group. Significant differences between two groups were assessed using Student's *t*-test, while those among multiple groups were assessed using a one-way analysis of variance followed by Dunnett's multiple comparisons test as a post hoc test. *$p<0.05$ vs. normal group, #$p<0.05$ vs. vehicle group

General Discussion

Chemokines comprise a superfamily of relatively small chemoattractant cytokines (Le et al. 2004). They have broad roles in human and animals, being involved in inflammation, allergic reactions, responses to tumors, etc. (Le et al. 2004). One of their most important roles is controlling immune responses (Le et al. 2004). Chemokine-targeted therapies thus may be effective for many disorders and diseases, but to be effective and safe, elucidation of the mechanisms of chemokine action will be necessary.

In the chapter 1, it was demonstrated that CXCL13 expressing LN- and PP-HEVs (Ebisuno et al. 2003) induce arrest in MLNs of B cells expressing CXCR5. In CXCL13-null mice, adhesion of B cells in MLN HEVs was selectively reduced, and this reduction was restored by the reconstitution of CXCL13 proteins in the MLN HEVs. In *in vitro* adhesion studies, CXCL13 induced shear-resistant B-cell adhesion under static and shear-stressed conditions by activation of integrins. CXCL13-induced integrin activation was Gαi-dependent and involved intracellular Rap1/RAPL-mediated signal pathways. These results corroborate previous observations in PP HEVs in CXCL13-null mice (Ebisuno et al. 2003) and show that

CXCL13 is an arrest chemokine for B cells in both MLN HEVs and PP HEVs. In addition to their critical roles in lymphocyte homing and recruitment to inflammatory sites, chemokines are involved in many other processes. CCL3 (MIP-1α), CXCL12 (SDF-1), CXCL2 (MIP-2α), CXCL8 (IL-8), and other CC, CXC, and CX3C chemokines act synergistically to regulate hematopoiesis (Broxmeyer et al. 1999, Ma et al. 1998). The CXCL12/CXCR4 axis plays an essential role in vascularization, haematopoiesis, and cerebellar development (Tachibana et al. 1998, Zou et al. 1998). CXCL8 is an essential protein in angiogenesis (Koch et al. 1992, Strieter et al. 1992).

Because of their involvement in immune system homeostasis and in development, dysfunction in chemokine signaling may be pathogenic. Chemokines such as CCL2, CCL5, CXCL8, and CXCL12 are involved in tumor growth and metastasis and as anti-tumor effectors, through induction of mononuclear cell migration to tumors (Wang et al. 1998, Murphy 2001). Murphy et al. (Murphy 2001) also have argued that CXCL12 functions as an arrest chemokine for CXCR4-expressing breast tumors. A mechanistic understanding of chemokines action thus is crucial if new treatments for tumor metastasis are to be developed. Additionally, as described in the chapter 1, CXCL13 expression at tumor sites promotes migration

of anti-tumor T cells expressing CXCR5 (Yang et al. 2021). Furthermore, anti-PD-1-directed tumor therapy is improved when done in combination with CXCL13. It is possible that chemokine add-on therapy also could be effective for tumors for which anti-PD-1 or anti-PD-L1 treatments are indicated (Yang et al. 2021). Chemokine control may also be of value in preventing viral infections as CCR5, a receptor for CCL5, is a co-receptor of HIV (Necula et al. 2021) and other chemokine receptors are involved in virus infection. These potential applications of drugs targeting chemokine signaling explain why the field is so active.

It is known that there are three FDA-approved drugs targeting chemokine signaling. Maraviroc (Selzentry; Pfizer) is a small-molecule blocker of HIV-1 entry into host cells mediated by the CCR5 chemokine receptor. This drug, in combination with other antiretroviral agents, was approved by the FDA and EMA in 2007 for combination anti-retroviral treatment of adults infected with only CCR5-tropic HIV-1 detectable and who have evidence of viral replication and HIV-1 strains resistant to multiple anti-retroviral agents. The mechanism of action of Maraviroc is unique because it blocks an HIV coreceptor (Moore et al. 2009, Stellbrink et al. 2016). Plerixafor (Mozobil; Genzyme) is an antagonist of CXCR4 that is used in combination with granulocyte-colony stimulating factor (G-CSF) to

mobilize haematopoietic stem cells to the peripheral blood for collection and subsequent autologous transplantation in patients with non-Hodgkin's lymphoma and multiple myeloma (DiPersio et al. 2009, Steinberg et al. 2010). Its mechanism of action is blocking the CXCL12/CXCR4 axis that plays a key role in haematopoietic stem cell homing and retention in the bone marrow. It is noteworthy that treatment of lymphomas with Plerixafor involves inhibiting a normal physiological function of CXCL12. Mogamulizmab is a monoclonal antibody for CCR4 that is used in the treatment of mycosis fungoides or Sézary syndrome (a T cell lymphoma) (Kim et al. 2018, Kasamon et al. 2019). In Sézary syndrome, its mechanism of action is thought to be binding to CCR4 over-expressed on the lymphoma cell surface, another action involving interference with normal physiologic functions. Given that pathophysiological roles of CCL2/CR2 axis in CKD which were shown in the Chapter 2 of the present study and several reports (Tang 1996, Natori 1997, Taniguchi 2007), the treatment approach of use of QC/iso QC inhibitors for CKD is considered similar to the concepts both of mogamulizmab (blocking pathophysiological function of atypically increased chemokine) and plerixafor (modulating chemotaxis of certain immune cells by blocking chemokine signaling).

In the chapter 2, effects of inhibition of CCL2/CCR2 axis was investigated as a novel therapeutic target by structurally destabilizing the chemokine protein using QC/isoQC inhibitors. Several reports of the potential therapeutic benefits of blocking the CCL2/CCR2 axis had been reported (Lloyd et al. 1997, Kitagawa et al. 2004, Kang et al. 2010, Sayyed et al. 2011) and some had already proceeded to clinical studies with CKD subjects. However, clinically meaningful benefits to the subjects were not observed. A randomized, double-blind, placebo-controlled clinical study with CCX140-B, a CCR2 inhibitor, has been conducted in subjects with type 2 diabetes and nephropathy (deZeeuw et al. 2015). Two doses of the drug (5 and 10 mg) were used. Surprisingly, only the lower dose showed statistically significant decreases in albuminuria at the completion of the study (56 weeks), although a trend toward effectiveness was seen at the higher dose. deZeeuw et al. further investigated this unexpected dose-dependency relationship. They reported that plasma CCL2 concentration increased in a dose dependent manner, which they suggested was a compensatory effect of CCL2/CCR2 inhibition and regarded as significant drawback of the CCL2/CCR2 inhibition approach for treatment of CKD. If so, development of CCR2 antagonists will require modifications to the approach and monitoring of plasma CCL2 levels.

In the chapter 2, it was also shown that chronic treatment of PQ529 decreased proteinuria and decreased CCL2 levels in blood, urine, and kidney. Decreases in proteinuria and CCL2 were correlated. These observations were not unexpected because the QC/isoQC inhibition approach results in the destabilization of CCL2 by blocking N-terminal pyroglutaminylation. Regardless of the previous failure of CCR2 antagonists, this novel approach thus seems effective and promising. Additionally, PQ529 reportedly showed therapeutic effects on other diseases such as *Staphylococcus aureus*-induced septic arthritis (Hellvard et al. 2013) and non-alcoholic fatty liver disease (Cynis et al. 2013) in animal studies, suggesting that the QC/isoQC inhibition approach may be a reasonable therapeutic approach to a wide variety of diseases with CCL2/CCR2 dysfunctions.

There is another anti-CCL2/CCR2 axis treatment, emapticap pegol (NOX-E36), which completed a phase 2 clinical study in type 2 diabetic patients with albuminuria (Menne et al. 2017). Emapticap pegol is an inhibitor of CCL2 that was administered to subjects for 12 weeks. Blood monocyte count was used as a pharmacodynamics biomarker, which decreased 15-20% during the study. However, only a trend toward reduction of albuminuria and HbA1c was observed at the end of the trial and thus far no additional studies have been reported. CCL2 levels were

significantly lower in blood (30%), urine (40%), and kidney (50%) at higher doses of emapticap pegol (100 mg/kg). This result may suggest higher potency of PQ529 than emaptical pegol, but as described in the chapter 2 as a limitation of the present study, blood monocyte count in chronic treatment of PQ529 has not been evaluated yet. The effect of PQ529 on proteinuria was larger in our non-clinical study than in the clinical trial of emapticap pegol, suggesting that PQ529 treatment may be superior, but translational studies will be required to determine if this true. Regardless, proteinuria may be a useful disease biomarker, as would CCL2 in blood and urine, that could be used in drug screening for CKD.

As described in the chapter 1, the mechanism of certain chemokines in lymphocyte homing is activation of adhesion molecules (e.g., integrin) expressed on the lymphocyte cell surface. It has been reported that CCL2 is an arrest chemokine for inflammation-induced monocyte migration to lymph nodes via HEVs (Palframan et al. 2001, Ley. 2003). Given this result, it has been hypothesized that overexpressed CCL2 in the glomerulonephritis kidney functions as an arrest chemokine to immobilize monocytes in glomeruli. To test this hypothesis, further investigation using blockers to adhesion molecules expressing on monocytes or HEVs would be helpful. α4 integrin expressed on monocytes (Yusuf-Makagiansar.

2002) also may contribute to monocyte migration to damaged glomeruli. This suggests another therapeutic approach for CKD, namely blocking integrin on monocytes. It is noted that vedolizumab, an anti-α4β7 integrin, is an FDA-approved drug for treating inflammatory bowel diseases (Luzentales-Simpson. 2021). This type of integrin inhibitor may also be effective for treating inflammatory kidney disease in CKD patients. Regardless of the mechanisms of action of different potential therapeutic agents, selectivity and specificity of the targeted molecules for glomerulonephritis will need to be established to ensure their safety and efficacy. For this purpose, as described in the chapter 2, will also be important to study further the involvement of chemokines other than CCL2 in the action of PQ529 in the glomerulonephritis rats, especially while the role of QC/isoQC in controlling the stability of other chemokines remains incomplete.

Collectively in the investigations of this dissertation, it was also suggested that there are multiple different types of effective and preferred approaches to modulate functions of a certain combination of chemokines and their receptors as novel treatments for diseases. In the chapter 1 and 2, it was described that physiological and pathophysiological functions of CXCL13/CXCR5 axis and CCL2/CCR5 axis are different. CXCL13 functions as a homeostatic chemokine,

and CCL2 show some pathophysiological functions under disease conditions. Regarding applications of CXCL13/CXCR5 axis for drug development, it has already suggested that the use of CXCL13 itself in combination with anti-PD-1 antibody, is effective on ovarian cancer (Yang et al. 2021). For enhancement of CXCL13/CXCR5, CXCR5 agonists or anti-CXCR5 agonistic antibodies may become potential therapeutic options, and further researches are warranted. In the chapter 2, it was suggested that promoting degradation of CCL2 by inhibition of QC/isoQC is effective and may overcome of drawbacks of other CCL2/CCR2 axis inhibition approaches such as increase of CCL2 after chronic treatment of a CCR2 inhibitor (deZeeuw et al. 2015) and marginal PD profile (Menne et al. 2017). Additionally, blockers to CCR5 (maraviroc) and CXCR4 (plexiafor) and anti-CCR4 monoclonal antibody (mogalizumab) have already been approved by the FDA for treatments of certain diseases. These evidences have implied that enhancement of homeostatic chemokines and inhibition of pathophysiological chemokines may be basic reasonable approaches for chemokine-based drug development. These also indicate that there should be different characteristics in multiple modalities to modulate chemokine/chemokine receptor axis enhancement or inhibition, and these differences relate to different outcomes even within the same target chemokine/chemokine receptor axis. This consideration also stresses importance of

confirmation of pharmacological signals in addition to pharmacokinetic and pharmacodynamic biomarkers of administered drugs in early nonclinical and clinical development (Morgan et al. 2012) to predict if the selected modality and approach may be the best approach to modulate the targeted chemokine signaling.

In summary, regarding the physiological function of chemokines in lymphocyte homing, it was shown that CXCL13 expressed on HEVs in lymph nodes is an arrest chemokine for B cells. This finding suggests therapeutic approaches to block functions of arrest chemokines in certain pathophysiological conditions. In CKD, it was shown that CCL2/CCR2 signaling is essential for the progression of glomerulonephritis by triggering monocyte mobilization into sites of inflammation. Inhibition of QC/isoQC was found to be effective in attenuating inflammation and dysfunction of the kidney by inhibiting this monocyte infiltration. QC/isoQC inhibition thus appear to be a novel and effective approach to manage glomerulonephritis and CKD.

Acknowledgements

I thank Drs. M. Miyasaka, T. Tanaka, and Y. Ebisuno for their advice and support during the preparation of this dissertation. I thank Dr. M. Okabe of the Research Institute for Microbial Diseases, Osaka University for the GFP-transgenic mice, Dr. Y. Iigo of Daiichi Pharmaceutical Co. for the rat ICAM-1/Ig, and Drs. T. Hirata and M. H. Jang for critically reading the manuscript. We also thank Ms. S. Yamashita and M. Komine for secretarial assistance and Ms. T. Kondo for technical help.

I thank Drs. Y. Tomura, M. Kashiwa, A. Tahara, Mrs. K. Schultz, Dr. L. Kovanda, and Mr. M. Takeuchi (Astellas Pharma Inc.) for their valuable comments and continuous encouragement regarding my research on QC/isoQC inhibitor (chapter 2) and on this dissertation. I also thank Mrs. F. Kiyonaga, Dr. Y. Mizukami, Mr. K. Maeno and T. Nishikubo, and Drs. H. Yoshida and H. Ito for their collaboration in this research.

I thank Profs. Y. Nakamura, A. Yoshiki, Associate Profs. D. Xu, M. O. Vilareal, Y. Miyamae, and Prof. H. Ito at the Doctoral Program of Life Science

Innovation, School of Integrated and Global Majors, the University of Tsukuba, for their advice, guidance, and coaching on my preparation for this doctoral dissertation.

List of Published Articles

Kanemitsu N, Ebisuno Y, Tanaka T, Otani K, Hayasaka H, Kaisho T, Akira S, Katagiri K, Kinashi T, Fujita N, Tsuruo T, Miyasaka M. CXCL13 is an arrest chemokine for B cells in high endothelial venules. *Blood*. 2005 Oct 15;106(8): 2613-8.

Kanemitsu N, Kiyonaga F, Mizukami K, Maeno K, Nishikubo T, Yoshida H, Ito H. Chronic treatment with the (iso-)glutaminyl cyclase inhibitor PQ529 is a novel and effective approach for glomerulonephritis in chronic kidney disease. *Naunyn Schmiedebergs Arch Pharmacol*. 2021 Apr;394(4): 751-61.

References

Ansel KM, Ngo VN, Hyman PL, Luther SA, Förster R, Sedgwick JD, Browning JL, Lipp M, Cyster JG. A chemokine-driven positive feedback loop organizes lymphoid follicles. *Nature*. 2000 Jul 20;406(6793): 309-14.

Banba N, Nakamura T, Matsumura M, Kuroda H, Hattori Y, Kasai K. Possible relationship of monocyte chemoattractant protein-1 with diabetic nephropathy. *Kidney Int*. 2000 Aug;58(2): 684-90.

Berl T. Review: renal protection by inhibition of the renin-angiotensin-aldosterone system. *J Renin Angiotensin Aldosterone Syst*. 2009 Mar;10(1): 1-8.

Broxmeyer HE, Kim CH. Regulation of hematopoiesis in a sea of chemokine family members with a plethora of redundant activities. *Exp Hematol*. 1999 Jul;27(7): 1113-23.

Broxmeyer HE, Kim CH, Cooper SH, Hangoc G, Hromas R, Pelus LM. Effects of CC, CXC, C, and CX3C chemokines on proliferation of myeloid progenitor cells, and insights into SDF-1-induced chemotaxis of progenitors. *Ann N Y Acad Sci*. 1999 Apr 30;872: 142-62; discussion 163.

Campbell JJ, Hedrick J, Zlotnik A, Siani MA, Thompson DA, Butcher EC. Chemokines and the arrest of lymphocytes rolling under flow conditions. *Science*. 1998 Jan 16;279(5349): 381-4.

Carr MW, Roth SJ, Luther E, Rose SS, Springer TA. Monocyte chemoattractant protein 1 acts as a T-lymphocyte chemoattractant. *Proc Natl Acad Sci U S A*. 1994 Apr 26;91(9): 3652-6.

Castan L, Magnan A, Bouchaud G. Chemokine receptors in allergic diseases. *Allergy*. 2017 May;72(5): 682-90.

Cecchinato V, D'Agostino G, Raeli L, Uguccioni M. Chemokine interaction with synergy-inducing molecules: fine tuning modulation of cell trafficking. *J Leukoc Biol*. 2016 Jun;99(6): 851-5.

Chen K, Bao Z, Tang P, Gong W, Yoshimura T, Wang JM. Chemokines in homeostasis and diseases. *Cell Mol Immunol*. 2018 Apr;15(4): 324-34.

Chen YL, Huang KF, Kuo WC, Lo YC, Lee YM, Wang AH. Inhibition of glutaminyl cyclase attenuates cell migration modulated by monocyte chemoattractant proteins. *Biochem J*. 2012 Mar 1;442(2): 403-12.

Cheng W, Chen G. Chemokines and chemokine receptors in multiple sclerosis. *Mediators Inflamm*. 2014;2014: 659206.

Cupedo T, Vondenhoff MF, Heeregrave EJ, De Weerd AE, Jansen W, Jackson DG, Kraal G, Mebius RE. Presumptive lymph node organizers are differentially represented in developing mesenteric and peripheral nodes. *J Immunol*. 2004 Sep 1;173(5): 2968-75.

Cynis H, Hoffmann T, Friedrich D, Kehlen A, Gans K, Kleinschmidt M, Rahfeld JU, Wolf R, Wermann M, Stephan A, Haegele M, Sedlmeier R, Graubner S, Jagla W, Müller A, Eichentopf R, Heiser U, Seifert F, Quax PH, de Vries MR, Hesse I, Trautwein D, Wollert U, Berg S, Freyse EJ, Schilling S, Demuth HU. The isoenzyme of glutaminyl cyclase is an important regulator of monocyte infiltration under inflammatory conditions. *EMBO Mol Med*. 2011 Sep;3(9): 545-58.

Cynis H, Kehlen A, Haegele M, Hoffmann T, Heiser U, Fujii M, Shibazaki Y, Yoneyama H, Schilling S, Demuth HU. Inhibition of Glutaminyl Cyclases alleviates CCL2-mediated inflammation of non-alcoholic fatty liver disease in mice. *Int J Exp Pathol*. 2013 Jun;94(3): 217-25.

Cynis H, Rahfeld JU, Stephan A, Kehlen A, Koch B, Wermann M, Demuth HU, Schilling S. Isolation of an isoenzyme of human glutaminyl cyclase: retention in the Golgi complex suggests involvement in the protein maturation machinery. *J Mol Biol*. 2008 Jun 20;379(5): 966-80.

de Zeeuw D, Bekker P, Henkel E, Hasslacher C, Gouni-Berthold I, Mehling H, Potarca A, Tesar V, Heerspink HJ, Schall TJ; CCX140-B Diabetic Nephropathy Study Group. The effect of CCR2 inhibitor CCX140-B on residual albuminuria in patients with type 2 diabetes and nephropathy: a randomised trial. *Lancet Diabetes Endocrinol*. 2015 Sep;3(9): 687-96.

DiPersio JF, Uy GL, Yasothan U, Kirkpatrick P. Plerixafor. *Nat Rev Drug Discov*. 2009 Feb;8(2): 105-6.

Disis ML, Taylor MH, Kelly K, Beck JT, Gordon M, Moore KM, Patel MR, Chaves J, Park H, Mita AC, Hamilton EP, Annunziata CM, Grote HJ, von Heydebreck A, Grewal J, Chand V, Gulley JL. Efficacy and Safety of Avelumab for Patients With Recurrent or Refractory Ovarian Cancer: Phase 1b Results From the JAVELIN Solid Tumor Trial. *JAMA Oncol*. 2019 Mar 1;5(3): 393-401.

Eardley KS, Zehnder D, Quinkler M, Lepenies J, Bates RL, Savage CO, Howie AJ, Adu D, Cockwell P. The relationship between albuminuria, MCP-1/CCL2, and interstitial macrophages in chronic kidney disease. *Kidney Int*. 2006 Apr;69(7): 1189-97.

Ebisuno Y, Tanaka T, Kanemitsu N, Kanda H, Yamaguchi K, Kaisho T, Akira S, Miyasaka M. Cutting edge: the B cell chemokine CXC chemokine ligand 13/B lymphocyte chemoattractant is expressed in the high endothelial venules of

lymph nodes and Peyer's patches and affects B cell trafficking across high endothelial venules. *J Immunol*. 2003 Aug 15;171(4): 1642-6.

Gao J, Liu X, Wei L, Niu D, Wei J, Wang L, Ge H, Wang M, Yu Q, Jin T, Tian T, Dai Z, Fu R. Genetic variants of MCP-1 and CCR2 genes and IgA nephropathy risk. *Oncotarget*. 2016 Nov 22;7(47): 77950-57.

Giunti S, Barutta F, Perin PC, Gruden G. Targeting the MCP-1/CCR2 System in diabetic kidney disease. *Curr Vasc Pharmacol*. 2010 Nov;8(6): 849-60.

Griffith JW, Sokol CL, Luster AD. Chemokines and chemokine receptors: positioning cells for host defense and immunity. *Annu Rev Immunol*. 2014;32: 659-702.

Gschwandtner M, Derler R, Midwood KS. More Than Just Attractive: How CCL2 Influences Myeloid Cell Behavior Beyond Chemotaxis. *Front Immunol*. 2019 Dec 13;10: 2759.

Gunn MD, Ngo VN, Ansel KM, Ekland EH, Cyster JG, Williams LT. A B-cell-homing chemokine made in lymphoid follicles activates Burkitt's lymphoma receptor-1. *Nature*. 1998 Feb 19;391(6669): 799-803.

Haller H, Bertram A, Nadrowitz F, Menne J. Monocyte chemoattractant protein-1 and the kidney. *Curr Opin Nephrol Hypertens*. 2016 Jan;25(1): 42-9.

Hamanishi J, Mandai M, Iwasaki M, Okazaki T, Tanaka Y, Yamaguchi K, Higuchi T, Yagi H, Takakura K, Minato N, Honjo T, Fujii S. Programmed cell death 1 ligand 1 and tumor-infiltrating CD8+ T lymphocytes are prognostic factors of human ovarian cancer. *Proc Natl Acad Sci U S A*. 2007 Feb 27;104(9): 3360-5.

Hellvard A, Maresz K, Schilling S, Graubner S, Heiser U, Jonsson R, Cynis H, Demuth HU, Potempa J, Mydel P. Glutaminyl cyclases as novel targets for the treatment of septic arthritis. *J Infect Dis*. 2013 Mar 1;207(5): 768-77.

Hodgkins KS, Schnaper HW. Tubulointerstitial injury and the progression of chronic kidney disease. *Pediatr Nephrol*. 2012 Jun;27(6): 901-9.

Huang Y, Caputo CR, Noordmans GA, Yazdani S, Monteiro LH, van den Born J, van Goor H, Heeringa P, Korstanje R, Hillebrands JL. Identification of novel genes associated with renal tertiary lymphoid organ formation in aging mice. *PLoS One*. 2014 Mar 17;9(3): e91850.

Hussain M, Adah D, Tariq M, Lu Y, Zhang J, Liu J. CXCL13/CXCR5 signaling axis in cancer. *Life Sci*. 2019 Jun 15;227: 175-86.

Iizuka T, Tanaka T, Suematsu M, Miura S, Watanabe T, Koike R, Ishimura Y, Ishii H, Miyasaka N, Miyasaka M. Stage-specific expression of mucosal addressin

cell adhesion molecule-1 during embryogenesis in rats. *J Immunol*. 2000 Mar 1;164(5): 2463-71.

Kasamon YL, Chen H, de Claro RA, Nie L, Ye J, Blumenthal GM, Farrell AT, Pazdur R. FDA Approval Summary: Mogamulizumab-kpkc for Mycosis Fungoides and Sézary Syndrome. *Clin Cancer Res*. 2019 Dec 15;25(24): 7275-80.

Katagiri K, Maeda A, Shimonaka M, Kinashi T. RAPL, a Rap1-binding molecule that mediates Rap1-induced adhesion through spatial regulation of LFA-1. *Nat Immunol*. 2003 Aug;4(8): 741-8.

Katagiri K, Ohnishi N, Kabashima K, Iyoda T, Takeda N, Shinkai Y, Inaba K, Kinashi T. Crucial functions of the Rap1 effector molecule RAPL in lymphocyte and dendritic cell trafficking. *Nat Immunol*. 2004 Oct;5(10): 1045-51.

Kang YS, Lee MH, Song HK, Ko GJ, Kwon OS, Lim TK, Kim SH, Han SY, Han KH, Lee JE, Han JY, Kim HK, Cha DR. CCR2 antagonism improves insulin resistance, lipid metabolism, and diabetic nephropathy in type 2 diabetic mice. *Kidney Int*. 2010 Nov;78(9): 883-94.

Kim YH, Bagot M, Pinter-Brown L, Rook AH, Porcu P, Horwitz SM, Whittaker S, Tokura Y, Vermeer M, Zinzani PL, Sokol L, Morris S, Kim EJ, Ortiz-Romero

PL, Eradat H, Scarisbrick J, Tsianakas A, Elmets C, Dalle S, Fisher DC, Halwani A, Poligone B, Greer J, Fierro MT, Khot A, Moskowitz AJ, Musiek A, Shustov A, Pro B, Geskin LJ, Dwyer K, Moriya J, Leoni M, Humphrey JS, Hudgens S, Grebennik DO, Tobinai K, Duvic M; MAVORIC Investigators. Mogamulizumab versus vorinostat in previously treated cutaneous T-cell lymphoma (MAVORIC): an international, open-label, randomised, controlled phase 3 trial. *Lancet Oncol*. 2018 Sep;19(9): 1192-204.

Kitagawa K, Wada T, Furuichi K, Hashimoto H, Ishiwata Y, Asano M, Takeya M, Kuziel WA, Matsushima K, Mukaida N, Yokoyama H. Blockade of CCR2 ameliorates progressive fibrosis in kidney. *Am J Pathol*. 2004 Jul;165(1): 237-46.

Koch AE, Polverini PJ, Kunkel SL, Harlow LA, DiPietro LA, Elner VM, Elner SG, Strieter RM. Interleukin-8 as a macrophage-derived mediator of angiogenesis. *Science*. 1992 Dec 11;258(5089): 1798-801.

Lambers Heerspink HJ, de Zeeuw D. Novel drugs and intervention strategies for the treatment of chronic kidney disease. *Br J Clin Pharmacol*. 2013 Oct;76(4): 536-50.

Le Y, Zhou Y, Iribarren P, Wang J. Chemokines and chemokine receptors: their manifold roles in homeostasis and disease. *Cell Mol Immunol*. 2004 Apr;1(2): 95-104.

Ley K. Arrest chemokines. *Microcirculation*. 2003 Jun;10(3-4): 289-95.

Ling MF, Luster AD. Novel approach to inhibiting chemokine function. *EMBO Mol Med*. 2011 Sep;3(9): 510-2.

Lloyd CM, Minto AW, Dorf ME, Proudfoot A, Wells TN, Salant DJ, Gutierrez-Ramos JC. RANTES and monocyte chemoattractant protein-1 (MCP-1) play an important role in the inflammatory phase of crescentic nephritis, but only MCP-1 is involved in crescent formation and interstitial fibrosis. *J Exp Med*. 1997 Apr 7;185(7): 1371-80.

López-Novoa JM, Martínez-Salgado C, Rodríguez-Peña AB, López-Hernández FJ. Common pathophysiological mechanisms of chronic kidney disease: therapeutic perspectives. *Pharmacol Ther*. 2010 Oct;128(1): 61-81.

Luzentales-Simpson M, Pang YCF, Zhang A, Sousa JA, Sly LM. Vedolizumab: Potential Mechanisms of Action for Reducing Pathological Inflammation in Inflammatory Bowel Diseases. *Front Cell Dev Biol*. 2021 Feb 3;9: 612830.

Ma Q, Jones D, Borghesani PR, Segal RA, Nagasawa T, Kishimoto T, Bronson RT, Springer TA. Impaired B-lymphopoiesis, myelopoiesis, and derailed

cerebellar neuron migration in CXCR4- and SDF-1-deficient mice. *Proc Natl Acad Sci U S A*. 1998 Aug 4;95(16): 9448-53.

Macconi D. Targeting the renin angiotensin system for remission/regression of chronic kidney disease. *Histol Histopathol*. 2010 May;25(5): 655-68.

McLeod SJ, Li AH, Lee RL, Burgess AE, Gold MR. The Rap GTPases regulate B cell migration toward the chemokine stromal cell-derived factor-1 (CXCL12): potential role for Rap2 in promoting B cell migration. *J Immunol*. 2002 Aug 1;169(3): 1365-71.

Menne J, Eulberg D, Beyer D, Baumann M, Saudek F, Valkusz Z, Więcek A, Haller H; Emapticap Study Group. C-C motif-ligand 2 inhibition with emapticap pegol (NOX-E36) in type 2 diabetic patients with albuminuria. *Nephrol Dial Transplant*. 2017 Feb 1;32(2): 307-315.

Miao M, De Clercq E, Li G. Clinical significance of chemokine receptor antagonists. *Expert Opin Drug Metab Toxicol*. 2020 Jan;16(1): 11-30.

Miyake K, Weissman IL, Greenberger JS, Kincade PW. Evidence for a role of the integrin VLA-4 in lympho-hemopoiesis. *J Exp Med*. 1991 Mar 1;173(3): 599-607.

Miyasaka M, Tanaka T. Lymphocyte trafficking across high endothelial venules: dogmas and enigmas. *Nat Rev Immunol*. 2004 May;4(5): 360-70.

Moadab F, Khorramdelazad H, Abbasifard M. Role of CCL2/CCR2 axis in the immunopathogenesis of rheumatoid arthritis: Latest evidence and therapeutic approaches. *Life Sci*. 2021 Mar 15;269: 119034.

Moore JP, Kuritzkes DR. A pièce de resistance: how HIV-1 escapes small molecule CCR5 inhibitors. *Curr Opin HIV AIDS*. 2009 Mar;4(2): 118-24.

Moreno JA, Gomez-Guerrero C, Mas S, Sanz AB, Lorenzo O, Ruiz-Ortega M, Opazo L, Mezzano S, Egido J. Targeting inflammation in diabetic nephropathy: a tale of hope. *Expert Opin Investig Drugs*. 2018 Nov;27(11): 917-30.

Morgan P, Van Der Graaf PH, Arrowsmith J, Feltner DE, Drummond KS, Wegner CD, Street SD. Can the flow of medicines be improved? Fundamental pharmacokinetic and pharmacological principles toward improving Phase II survival. *Drug Discov Today*. 2012 May;17(9-10): 419-24.

Moser B, Ebert L. Lymphocyte traffic control by chemokines: follicular B helper T cells. *Immunol Lett*. 2003 Jan 22;85(2): 105-12.

Mukasa R, Satoh A, Tominaga Y, Yamazaki M, Matsumoto K, Iigo Y, Higashida T, Kita Y, Miyasaka M, Takashi T. Development of a cell-free binding assay for rat ICAM-1/LFA-1 interactions using a novel anti-rat LFA-1 monoclonal

antibody and comparison with a cell-based assay. *J Immunol Methods*. 1999 Aug 31;228(1-2): 69-79.

Murphy PM. Chemokines and the molecular basis of cancer metastasis. *N Engl J Med*. 2001 Sep 13;345(11): 833-5.

Nagarsheth N, Wicha MS, Zou W. Chemokines in the cancer microenvironment and their relevance in cancer immunotherapy. *Nat Rev Immunol*. 2017 Sep;17(9): 559-72.

Nakano H, Gunn MD. Gene duplications at the chemokine locus on mouse chromosome 4: multiple strain-specific haplotypes and the deletion of secondary lymphoid-organ chemokine and EBI-1 ligand chemokine genes in the *plt* mutation. *J Immunol*. 2001 Jan 1;166(1): 361-9.

Natori Y, Sekiguchi M, Ou Z, Natori Y. Gene expression of CC chemokines in experimental crescentic glomerulonephritis (CGN). *Clin Exp Immunol*. 1997 Jul;109(1): 143-8.

Necula D, Riviere-Cazaux C, Shen Y, Zhou M. Insight into the roles of CCR5 in learning and memory in normal and disordered states. *Brain Behav Immun*. 2021 Feb;92: 1-9.

Nishimura T, Itoh T. Higher level expression of lymphocyte function-associated antigen-1 (LFA-1) on *in vivo* natural killer cells. *Eur J Immunol*. 1988 Dec;18(12): 2077-80.

Okabe M, Ikawa M, Kominami K, Nakanishi T, Nishimune Y. 'Green mice' as a source of ubiquitous green cells. *FEBS Lett*. 1997 May 5;407(3): 313-9.

Okada T, Ngo VN, Ekland EH, Förster R, Lipp M, Littman DR, Cyster JG. Chemokine requirements for B cell entry to lymph nodes and Peyer's patches. *J Exp Med*. 2002 Jul 1;196(1): 65-75.

Palframan RT, Jung S, Cheng G, Weninger W, Luo Y, Dorf M, Littman DR, Rollins BJ, Zweerink H, Rot A, von Andrian UH. Inflammatory chemokine transport and presentation in HEV: a remote control mechanism for monocyte recruitment to lymph nodes in inflamed tissues. *J Exp Med*. 2001 Nov 5;194(9): 1361-73.

Perez-Gomez MV, Sanchez-Niño MD, Sanz AB, Zheng B, Martín-Cleary C, Ruiz-Ortega M, Ortiz A, Fernandez-Fernandez B. Targeting inflammation in diabetic kidney disease: early clinical trials. *Expert Opin Investig Drugs*. 2016 Sep;25(9): 1045-58.

Reedquist KA, Bos JL. Costimulation through CD28 suppresses T cell receptor-dependent activation of the Ras-like small GTPase Rap1 in human T lymphocytes. *J Biol Chem*. 1998 Feb 27;273(9): 4944-9.

Rot A, von Andrian UH. Chemokines in innate and adaptive host defense: basic chemokinese grammar for immune cells. *Annu Rev Immunol*. 2004;22: 891-928.

Sayyed SG, Ryu M, Kulkarni OP, Schmid H, Lichtnekert J, Grüner S, Green L, Mattei P, Hartmann G, Anders HJ. An orally active chemokine receptor CCR2 antagonist prevents glomerulosclerosis and renal failure in type 2 diabetes. *Kidney Int*. 2011 Jul;80(1): 68-78.

Schaerli P, Willimann K, Lang AB, Lipp M, Loetscher P, Moser B. CXC chemokine receptor 5 expression defines follicular homing T cells with B cell helper function. *J Exp Med*. 2000 Dec 4;192(11): 1553-62.

Schulz O, Hammerschmidt SI, Moschovakis GL, Förster R. Chemokines and Chemokine Receptors in Lymphoid Tissue Dynamics. *Annu Rev Immunol*. 2016 May 20;34: 203-42.

Shamri R, Grabovsky V, Feigelson SW, Dwir O, Van Kooyk Y, Alon R. Chemokine stimulation of lymphocyte alpha 4 integrin avidity but not of leukocyte function-associated antigen-1 avidity to endothelial ligands under

shear flow requires cholesterol membrane rafts. *J Biol Chem*. 2002 Oct 18;277(42): 40027-35.

Shimonaka M, Katagiri K, Nakayama T, Fujita N, Tsuruo T, Yoshie O, Kinashi T. Rap1 translates chemokine signals to integrin activation, cell polarization, and motility across vascular endothelium under flow. *J Cell Biol*. 2003 Apr 28;161(2): 417-27.

Siddiqui K, Joy SS, Al-Rubeaan K. Association of urinary monocyte chemoattractant protein-1 (MCP-1) and kidney injury molecule-1 (KIM-1) with risk factors of diabetic kidney disease in type 2 diabetes patients. *Int Urol Nephrol*. 2019 Aug;51(8): 1379-86.

Solari R, Pease JE, Begg M. "Chemokine receptors as therapeutic targets: Why aren't there more drugs?". *Eur J Pharmacol*. 2015 Jan 5;746: 363-7.

Stasikowska O, Wagrowska-Danilewicz M. Chemokines and chemokine receptors in glomerulonephritis and renal allograft rejection. *Med Sci Monit*. 2007 Feb;13(2): RA31-6.

Stein JV, Rot A, Luo Y, Narasimhaswamy M, Nakano H, Gunn MD, Matsuzawa A, Quackenbush EJ, Dorf ME, von Andrian UH. The CC chemokine thymus-derived chemotactic agent 4 (TCA-4, secondary lymphoid tissue chemokine, 6Ckine, exodus-2) triggers lymphocyte function-associated antigen 1-

mediated arrest of rolling T lymphocytes in peripheral lymph node high endothelial venules. *J Exp Med*. 2000 Jan 3;191(1): 61-76.

Steinberg M, Silva M. Plerixafor: A chemokine receptor-4 antagonist for mobilization of hematopoietic stem cells for transplantation after high-dose chemotherapy for non-Hodgkin's lymphoma or multiple myeloma. *Clin Ther*. 2010 May;32(5): 821-43.

Stellbrink HJ, Le Fevre E, Carr A, Saag MS, Mukwaya G, Nozza S, Valluri SR, Vourvahis M, Rinehart AR, McFadyen L, Fichtenbaum C, Clark A, Craig C, Fang AF, Heera J. Once-daily maraviroc versus tenofovir/emtricitabine each combined with darunavir/ritonavir for initial HIV-1 treatment. *AIDS*. 2016 May 15;30(8): 1229-38.

Streeter PR, Berg EL, Rouse BT, Bargatze RF, Butcher EC. A tissue-specific endothelial cell molecule involved in lymphocyte homing. *Nature*. 1988 Jan 7;331(6151): 41-6.

Strieter RM, Kunkel SL, Elner VM, Martonyi CL, Koch AE, Polverini PJ, Elner SG. Interleukin-8. A corneal factor that induces neovascularization. *Am J Pathol*. 1992 Dec;141(6): 1279-84.

Tachibana K, Hirota S, Iizasa H, Yoshida H, Kawabata K, Kataoka Y, Kitamura Y, Matsushima K, Yoshida N, Nishikawa S, Kishimoto T, Nagasawa T. The

chemokine receptor CXCR4 is essential for vascularization of the gastrointestinal tract. *Nature*. 1998 Jun 11;393(6685): 591-4.

Tamatani T, Miyasaka M. Identification of monoclonal antibodies reactive with the rat homolog of ICAM-1, and evidence for a differential involvement of ICAM-1 in the adherence of resting versus activated lymphocytes to high endothelial cells. *Int Immunol*. 1990;2(2): 165-71.

Tampe D, Zeisberg M. Potential approaches to reverse or repair renal fibrosis. *Nat Rev Nephrol*. 2014 Apr;10(4): 226-37.

Taniguchi H, Kojima R, Sade H, Furuya M, Inomata N, Ito M. Involvement of MCP-1 in tubulointerstitial fibrosis through massive proteinuria in anti-GBM nephritis induced in WKY rats. *J Clin Immunol*. 2007 Jul;27(4): 409-29.

Tang WW, Qi M, Warren JS. Monocyte chemoattractant protein 1 mediates glomerular macrophage infiltration in anti-GBM Ab GN. *Kidney Int*. 1996 Aug;50(2): 665-71.

Tesch GH, Schwarting A, Kinoshita K, Lan HY, Rollins BJ, Kelley VR. Monocyte chemoattractant protein-1 promotes macrophage-mediated tubular injury, but not glomerular injury, in nephrotoxic serum nephritis. *J Clin Invest*. 1999 Jan;103(1): 73-80.

Verhave JC, Bouchard J, Goupil R, Pichette V, Brachemi S, Madore F, Troyanov S. Clinical value of inflammatory urinary biomarkers in overt diabetic nephropathy: a prospective study. *Diabetes Res Clin Pract*. 2013 Sep;101(3): 333-40.

Viedt C, Dechend R, Fei J, Hänsch GM, Kreuzer J, Orth SR. MCP-1 induces inflammatory activation of human tubular epithelial cells: involvement of the transcription factors, nuclear factor-kappaB and activating protein-1. *J Am Soc Nephrol*. 2002 Jun;13(6): 1534-47.

Wada T, Yokoyama H, Furuichi K, Kobayashi KI, Harada K, Naruto M, Su SB, Akiyama M, Mukaida N, Matsushima K. Intervention of crescentic glomerulonephritis by antibodies to monocyte chemotactic and activating factor (MCAF/MCP-1). *FASEB J*. 1996 Oct;10(12): 1418-25.

Wada T, Furuichi K, Sakai N, Iwata Y, Yoshimoto K, Shimizu M, Takeda SI, Takasawa K, Yoshimura M, Kida H, Kobayashi KI, Mukaida N, Naito T, Matsushima K, Yokoyama H. Up-regulation of monocyte chemoattractant protein-1 in tubulointerstitial lesions of human diabetic nephropathy. *Kidney Int*. 2000 Oct;58(4): 1492-9.

Wang JM, Deng X, Gong W, Su S. Chemokines and their role in tumor growth and metastasis. *J Immunol Methods*. 1998 Nov 1;220(1-2): 1-17.

Warnock RA, Campbell JJ, Dorf ME, Matsuzawa A, McEvoy LM, Butcher EC. The role of chemokines in the microenvironmental control of T versus B cell arrest in Peyer's patch high endothelial venules. *J Exp Med*. 2000 Jan 3;191(1): 77-88.

Xu LL, Warren MK, Rose WL, Gong W, Wang JM. Human recombinant monocyte chemotactic protein and other C-C chemokines bind and induce directional migration of dendritic cells *in vitro*. *J Leukoc Biol*. 1996 Sep;60(3): 365-71.

Yang M, Lu J, Zhang G, Wang Y, He M, Xu Q, Xu C, Liu H. CXCL13 shapes immunoactive tumor microenvironment and enhances the efficacy of PD-1 checkpoint blockade in high-grade serous ovarian cancer. *J Immunother Cancer*. 2021 Jan;9(1): e001136.

Yonemoto S, Machiguchi T, Nomura K, Minakata T, Nanno M, Yoshida H. Correlations of tissue macrophages and cytoskeletal protein expression with renal fibrosis in patients with diabetes mellitus. *Clin Exp Nephrol*. 2006 Sep;10(3): 186-92.

Yusuf-Makagiansar H, Anderson ME, Yakovleva TV, Murray JS, Siahaan TJ. Inhibition of LFA-1/ICAM-1 and VLA-4/VCAM-1 as a therapeutic approach to inflammation and autoimmune diseases. *Med Res Rev*. 2002 Mar;22(2): 146-67.

Zhang Y, Fujita N, Oh-hara T, Morinaga Y, Nakagawa T, Yamada M, Tsuruo T. Production of interleukin-11 in bone-derived endothelial cells and its role in the formation of osteolytic bone metastasis. *Oncogene*. 1998 Feb 12;16(6): 693-703.

Zou YR, Kottmann AH, Kuroda M, Taniuchi I, Littman DR. Function of the chemokine receptor CXCR4 in haematopoiesis and in cerebellar development. *Nature*. 1998 Jun 11;393(6685): 595-9.